

IDENTIFICATION OF OPTIMUM MILLING PARAMETERS
THROUGH MACHINE LEARNING

by

GAMZE BALÇIK

Submitted to the Graduate School of Engineering and Natural Sciences
in partial fulfillment of the requirements for the degree of
Master of Science

Sabancı University

Fall 2024

© Gamze Balçık 2024

All Rights Reserved

ABSTRACT

Milling operations are commonly utilized in many industries. Productivity rate becomes prominent in the industries such as automotive due to the need for high-volume manufacturing or the requirement to produce large die casts, whereas the aerospace and electronics industry must focus on precise manufacturing that does not exceed tolerance bands. This condition results in different types of optimization equations such as maximizing material removal rate with respect to machining center limits or minimizing the tool deflection and chatter risk to achieve conforming parts. Both optimizations will indicate a major effect on the unit cost of the product, hence they should describe the trade-off between the machining time and tool cost and help the selection of the optimum cutting parameters and tool dimensions.

The increase in AI implementations and their promising accuracy levels were the main reasons to choose the supervised machine learning (ML) to investigate the optimum solution. In this thesis, Titanium alloy (Ti-6-4) workpiece material cutting process with carbide tool has been simulated for many different cutting tool and process parameter scenarios to calculate cutting forces, chatter status, surface form errors, machining time, tool life and tool breakage. Following the data preparation step, Gaussian Process Regression model has been computed for the optimization step with Bayesian approach.

Keywords: Milling, Bayesian Optimization, Machine Learning

ÖZET

Frezeleme işlemleri birçok endüstride yaygın olarak kullanılmaktadır. Otomotiv gibi endüstrilerde, yüksek hacimli imalat ihtiyacı veya büyük kalıpların üretilmesi gerekliliği nedeniyle üretim hızı öne çıkarken, havacılık ve elektronik endüstrileri tolerans bantlarını aşmayan hassas imalata odaklanmak zorundadır. Bu durum, işleme merkezi sınırları dahilinde malzeme kaldırma oranını maksimize etmek veya kabul edilebilir parçalar elde etmek için takım sapması ve titreşim riskini minimize etmek gibi farklı optimizasyon denklemleri gerektirir. Her iki optimizasyon da ürünün birim maliyeti üzerinde büyük bir etki yaratacağından, işleme süresi ile takım maliyeti arasındaki dengeyi tanımlamalı ve optimum kesme parametreleri ile takım boyutlarının seçimine yardımcı olunmalıdır.

Bu tezde, yapay zeka uygulamalarındaki artış ve tahminlerdeki doğruluk seviyeleri nedeniyle, optimum çözüm, denetimli makine öğrenimini (ML) ile araştırıldı. Titanyum alaşımı (Ti-6-4) iş parçası malzemesinin karbür takım ile kesme işlemi, farklı kesici takım ve parametre senaryolarıyla simüle edilerek kesme kuvvetleri, titreşim durumu, yüzey hataları, işleme süresi, takım ömrü ve takım bükülme stresi hesaplanmıştır. Veri hazırlama adımının ardından, verileri test etmek ve eğitmek için Gauss Süreci regresyonu kullanılmış, Bayes Optimizasyonu ile en iyi sonuçlar belirlenmiştir.

Anahtar Kelimeler: Frezeleme, Bayesçi Eniyileme, Makine Öğrenmesi

*To my mom,
who put me into pressurized die cast process
to get a very strong woman at any cost
I was like air, she made me solid.
In the end I could brew them both
Now I am in my liquid phase
Flowing with life*

*To my love,
who thought me to bend not to break*

*To my kids,
So ordinary and so unique
At the same time
How come!*

ACKNOWLEDGEMENTS

I am deeply thankful to my thesis advisor, Prof. Dr. Erhan Budak, with whom we crossed twice. His very warm welcome after a sudden quit and 14-year break gave me the encourage to restart with amnesty law. I feel blessed to have an access to his expertise for both my professional and personal life. His supports and patience is of great contribution to my thesis completion.

I would kindly like to add my great appreciation to all members of MRL, especially Arash Ebrahimi, Faraz Tehranizadeh and Farzah Pashmforoush for their constructive supports and valuable accompany.

I definitely feel a huge gratitude to my husband for sharing the major responsibility of our kids during my thesis. His existence always helps me with my emotional regulation. My kids were very understanding eventhough they could hardly understand why I have to attend to courses at the age of 39.

I should thank to my mom, who always asks for more and more achievements. Her approach caused very deep feeling of inadequacy, however I could understand her source of trigger mechanism -after so many years- and convert it into positive progress power of my life. I have a little bit more to process :)

Finally, I want to thank me for proceeding with hugging all hard feelings and the mass of my mind, reading a lot to regulate my emotions and putting my attention into what is available rather than what is missing.

CONTENTS

1. INTRODUCTION	1
1.1 Literature Survey	3
1.2 Problem Definition	7
1.3 Methodology	8
2. DATA PREPARATION FOR MACHINE LEARNING	10
2.1 Cutting Forces	11
2.2 Form Error	15
2.3 Tool Life	18
2.4 Material Removal Rate (MRR).....	19
2.5 Tool Bending Stress.....	19
2.6 Power and Torque Consumption	20
2.7 Limits for Data Preparation	20
3. MACHINE LEARNING MODEL: GPR WITH BAYESIAN OPTIMIZATION	22
3.1 GPR and BO for all output variables	22
3.2 Acquisition Function.....	26
3.3 Model Performance.....	28
3.4 An alternative approach for Tool Life	32
3.5 Feature Importance and Residuals.....	34
4. OPTIMIZATION METHOD TO IDENTIFY OPTIMUM CUTTING PARAMETERS	37
4.1 Objective Function.....	37
4.2 Optimization Methods and Results.....	38
4.2.1 Genetic Algorithm for Multi Objective Optimization	40
4.2.2 Bayesian Optimization with Weight Definition	40
4.2.3 Non-linear Constrained Optimization.....	42
4.3 Constraint Definition	42
4.3.1 Feed per Tooth Limits.....	43
4.3.2 Power and Torque Limits of Machine Center	44
4.3.3 Axial Depth of Cut Limits	45

4.3.4 Radial Depth of Cut Limits.....	45
4.3.5 Spindle Speed Limits	46
4.3.6 FRF Measurement.....	46
4.3.7 Design Tolerance Limits.....	49
5. RESULTS	50
5.1 MULTI-OBJECTIVE OPTIMIZATION WITH GENETIC ALGORITHM.....	50
5.2 BAYESIAN OPTIMIZATION WITH EXPLICIT WEIGHT DEFINITION	53
5.3 WHEN TOOL LIFE HAS A MINIMUM MACHINING TIME	64
6. EXPERIMENTAL VERIFICATION.....	67
6.1 Cutting Tool.....	67
6.2 Parameter Selection for Testing.....	68
6.3 Measurements	69
6.3.1 Force Measurement.....	69
6.3.2 Tool Wear	73
6.3.3 Surface Roughness.....	74
7. CONCLUSION.....	77
REFERENCES	79

LIST OF FIGURES

Figure 1. Overall ML process schematic representation	8
Figure 2. f Flowchart of ML-based optimization for milling with maximum productivity .	10
Figure 3.The representation orthogonal cutting geometry.....	12
Figure 4: schematic representation of GPR	28
Figure 5: Comparison for MRR.....	29
Figure 6: Comparison for Tool Life	29
Figure 7: Comparison for Power	29
Figure 8: Comparison for Torque	29
Figure 9: Comparison for Tool Bending Stress	29
Figure 10: Comparison for Form Error.....	29
Figure 11: LS-Boost performance on Tool Life Prediction.....	33
Figure 12: Hone radius measurement using Nano-focus μ -surf explorer.....	43
Figure 13: Tool Catalog for Feed Rate Upper Limit	44
Figure 14. Power/torque curve of Mazak Nexus 510 CII Milling Center.	45
Figure 15: PCB Piezotronics Modal Analysis Sets	47
Figure 16. Stability lobe diagram	47
Figure 17. application of surface profile tolerance on a basic contour.....	49
Figure 18: The best Solutions Scatter Plot for Finishing Operation with WMRR=0, WTL=100 and min machining time limitation solved with Nonlinear Constrained Optimization	66
Figure 19: The cutting tool on machining center.....	67
Figure 20: Mazak Nexus 510 CII Milling Center (12.000rpm).....	69
Figure 21: Kistler Piezo-Dynamometer with Large Measuring Range	69
Figure 22: Cutting Force Plot	70
Figure 23: The Cutting Forces for Tool-Life Optimized Experiment	70
Figure 24: The Cutting Force Measurement for MRR-Optimized Test	71
Figure 25: The instrument to measure tool wear: Dino-Lite	73
Figure 26: Wear status of Tool-life optimized result.....	73
Figure 27: Wear status of MRR-optimized result.....	73

Figure 28: Surface Roughness measurement with KTaylor Hobson – Form Talysurf 50 ... 74
Figure 29: Surface Roughness result for Tool Life maximized solution.....75
Figure 30: Surface Roughness result for MRR optimized solution..... 75
Figure 31: Surface generation and Form Error for two optimized parameters..... 76

LIST OF TABLES

Table 1. Variable list of optimization problem.....	9
Table 2. Hyperparameters of Bayesian Optimization and Gaussian Process Regression	23
Table 3: Summary of ML performance metrics	23
Table 4: Selected Parameters of GPR process.....	27
Table 5: GPR Model Performance Results on Output Variables	28
Table 6: Actual vs Predicted Plots for Output Variables.....	29
Table 7: Convergence Plots of each Output Variable.....	32
Table 8: LS-Boost performance results for Tool Life	33
Table 9: Feature Importance and Residual Plots for each output variable	36
Table 10: Comparison of the Optimization Methods	39
Table 11: FRF Measurement Results to select chatter free solutions.....	48
Table 12: Roughing Solutions from Genetic Algorithm	53
Table 13: Finishing Solutions of Genetic Algorithm.....	53
Table 14. Best two optimal solutions per each normalization technique for a chatter-free roughing operation with different weight definitions	58
Table 15: Best Solutions Scatter Plot for Roughing Operation with $W_{MRR}=0$, $W_{TL}=100$	59
Table 16: Best Solutions Scatter Plot for Roughing Operation with $W_{MRR}=100$, $W_{TL}=0$	60
Table 17: Best two optimal solutions per each normalization technique for a chatter-free finishing operation with different weight definitions	61
Table 18: Best Solutions Scatter Plot for Finishing Operation with $W_{MRR}=0$, $W_{TL}=100$	62
Table 19: Best Solutions Scatter Plot for Finishing Operation with $W_{MRR}=100$, $W_{TL}=0$	63
Table 20: Best Solutions for Finishing Operation with min machining time constraint and $W_{MRR}=0$, $W_{TL}=100$ with different scaling techniques.....	64
Table 21: Best Solutions Scatter Plot for Finishing Operation with $W_{MRR}=0$, $W_{TL}=100$ and min machining time limitation solved with Bayesian Optimization	65
Table 22: The codes for the cutting tool	67
Table 23: Summary for Test Results for both MRR and Tool-Life Optimizes solutions	68
Table 24: The cutting force results of the experimental verification.....	72
Table 25: Surface Roughness comparison between Tool Life and MRR optimized results	76
Table 26: Surface Roughness comparison.....	76

1. Introduction

Milling is a widely used process in various industries and the complexity of this process still results in a major research area. The operation involves a rotating tool with cutting edges to remove metals or alloys by chip formation to obtain the designed geometry within the defined tolerance limits. Selection of each milling parameter such as feed rate, axial depth, radial depth, spindle speed without chatter generation, and tool related items as diameter, number of flutes and helix angle have major effects on machining time, tool cost, dimensional accuracy and surface quality. The trade-off between high production rate and acceptable dimensional accuracy is still a challenging optimization problem and traditionally selecting optimal machining parameters has relied heavily on the expertise and experience of skilled machinists, as well as on trial-and-error methods. However, these conventional approaches often result in suboptimal performance, increased production costs, and extended lead times.

The optimization process can be divided into two main categories: roughing and finishing operations. Both operations require different objective functions and constraints. Roughing operations target to complete the tool path with maximum material rate (MRR) to decrease machining time that leads to selecting the highest parameters regarding CNC center torque-power limitation. However, tool life and wear mechanism are pioneer limiting parameters since number of tools spent has a major effect on production cost. Tool changes during operation are not recommended due to mismatch marks on surface, but this can be neglected for roughing operations. Finishing operations refers to final surface generation, which affects the dimensional accuracy, and the conformance of the machined part. Especially aviation, aerospace and defense industries work with relatively tight tolerances with low production volumes and very expensive components can be rejected due to even 0.001-inch non-conformance values depending on related feature function in design. Hence, objective function regards max tool life subject to required form error.

Both roughing and finishing operation must avoid one critical occurrence: chatter vibrations, meaning that undesirable oscillations causing poor surface finish, tool breakage and damage on workpiece and machining center. Hence, optimization of machining parameters must always consider chatter mitigation. Currently, advanced technologies are available to generate stability lobe diagrams and identify stable cutting conditions. A hammer test on the cutting tool needs to be completed in advance to find out natural frequencies and mode shapes of the cutting tool.

The optimization process is based on true representation of cutting forces which requires a set of experiments to identify orthogonal database parameters to calculate cutting force coefficients of cutter-workpiece pair. The experiments require a complex set up including highly sensitive sensors and dynamometers, and detailed regression computations. These cutting forces are used for form error calculation.

Finally, tool life calculation is an important calculation of the objective function since it has a major effect on overall cost of the product, repeatability and sustainability of the process and good surface quality. For example, it is of great importance to complete the whole finishing process with only one tool because any mismatch on the part can result in rejection of the part and has a significant adverse effect on mechanical capability of the part.

The contribution of this thesis is to develop and solve an optimization model for both roughing and finishing operation that generates optimum cutting parameters without chatter by using hybrid approach that combines analytical calculations and experimental results with Machine Learning (ML) algorithms. Prior to optimization step, regression models of the machine learning are established with a promising performance for each output. This step requires a dataset to predict new datapoints. Regarding two main types of machine learning as supervised and unsupervised, the optimization problems are fitting to the supervised ML context. Among many supervised learning algorithms, Gaussian Process (GP) with Bayesian Optimization (BO) and Gradient Boosting model only for tool life have been selected to find the optimal parameters efficiently since both they are powerful tools for regression,

classification and optimization tasks as they define input-output relationships clearly and, a consistent, accurate and complete dataset is provided for predictions. The developed models have been solved with three different computational methods: genetic algorithm, Bayesian optimization and non-linear constrained approach after applying machine learning techniques to predict uncalculated parameters effectively without the need for extra testing. Genetic algorithm directly utilizes the multi-objective function with defined constraints to generate optimum solution(s) with a default equal weight definition. Bayesian optimization allows the machinist to define explicit weights with respect to different requirements of any process and it follows the weighted sum approach. The final approach, the non-linear constrained method, refers to one specific case, when the machining time needs to be longer than a specific timing requirement. This specific objective function can be additionally solved with Bayesian optimization. Among these methods, Bayesian approach is highlighted as the most promising approach.

1.1 Literature Survey

Optimum milling parameter selection is a major research area for increased productivity with minimum cost and enhanced quality. The repeatability and sustainability of the processes require a significant amount of engineering efforts since especially in aviation and aerospace industry, even 1-mil nonconformance on the parts forces all design analyses to be reassessed respectively for each feature for the acceptance and procurement. Any improvement in the machining of the part will have a decreasing effect on both manufacturing cost and design engineering effort and the number of rejected parts.

Traditional optimization studies refer to non-linear formulation of objective function with relevant constraints for both roughing and finishing operations. These studies suggest that optimizing depths of cut, attaching additional masses, and using multi-objective optimization models can significantly enhance chatter-free material removal rates in end milling, improving machining efficiency and quality [1]. Optimal selection of axial and radial

depths of cut pairs in milling maximizes chatter-free material removal, reducing machining time and improving productivity and part quality [2]. Ghani et al. suggested the optimal combination for low cutting force and good surface finish in end milling is high cutting speed, low feed rate, and low depth of cut, using the Taguchi optimization method [3]. Budak published a study an optimization method by using variable pitch cutter to mitigate from severe chatter conditions and excessive cutting forces was taken under control by an analytical approach that keeps a constant cutting force and updated feed rate instantly in G-Code [4]. Merdol and Altintas has studied the optimization and feed rate scheduling in two main streams: preprocess and postprocess optimization. Preprocess contained the calculations on maximizing MRR with chatter stability and torque/power constraints taking chip thinning affect into account. Post process optimization was focused on feed rate and spindle speed scheduling and G-code update for each line of NC tool path [5].

The rapid developments in Artificial Intelligence (AI) and Machine Learning (ML) have significantly transformed various industrial areas, including manufacturing. The number of publications about the optimum parameter selection using different ML approaches and regression methods are increasing since this approach is quite promising in making predictions with very few data by leveraging data-driven algorithms and modeling complex relationships with its powerful regression methods. For example, Karandikar et al. utilized Bayesian Optimization approach to predict the chatter probability of any cutting condition by setting up stability limit diagrams without knowing the tool point frequency response function and the cutting force coefficients [6].

Integrating mechanistic force models with ML provides accurate cutting force estimates for power/torque and form error calculations Tansel et al. demonstrated the effectiveness of combining cutting force predictions with neural network models for tool wear estimation in micro-milling [7]. Li and Chang developed an intelligent optimization system for machining parameters using ML, which underlines the practical benefits of such tools in real-world applications [8]. In addition to milling processes, Bertsimas and Dunn highlighted the broader applications of ML in optimization across various manufacturing processes, emphasizing its potential to revolutionize the industry [9].

Many different algorithms and optimizers are available in the machine learning area. ML approaches for regression models to predict new outcomes and optimizations are listed in Table 1. These methods and techniques can be used together. For example: Bayesian Optimization can tune hyperparameters of a Gaussian Process Regression (GPR) model or Particle Swarm Optimization (PSO) can optimize parameters in a Neural Network.

Regression Models	Optimization
Linear Models: Ridge, Lasso, Elastic Net and Bayesian Regression models	Gradient Based Methods
Non-Linear Models: Polynomial and generalized additive models	Bayesian Optimization with hyperparameter optimization
Tree Based Models: Decision trees, random forests and gradient boosted trees such as XGBoost and CatBoost	Evolutionary algorithms such as genetic algorithm or differential evolution
Support Vector Machines	Swarm intelligence methods: particle swarm or ant colony optimization
Kernel Based Methods as GPR	Simulated Annealing
Neural Network Models	Grid and Random Search
Ensemble Methods such as bagging, stacking or boosting regressors	Meta-heuristic and hybrid approaches, ie. Firefly algorithm or harmony search
Probabilistic models	Reinforcement Learning-Based optimization

Table 1: The list of ML regression and optimization methods

In this study, leveraging advanced algorithms like BO and GPR, an optimum parameter set is estimated that help manufacturers achieve efficient, cost-effective, high-quality outcomes, promising further enhancements in machining stability, precision, and automation [10]. Unlike traditional methods such as genetic algorithms and non-linear constrained, which can become inefficient in such scenarios, Bayesian Optimization leverages a probabilistic model to explore the parameter space more effectively. However, the results for these methods have been listed. By incorporating Gaussian process

regression as the surrogate model, the algorithm approximates the objective function and uses this approximation to guide the search for optimal solutions. This method not only helps in finding the best set of machining parameters but also provides a framework for systematically balancing competing objectives and constraints. The choice of Bayesian Optimization is particularly advantageous for achieving high performance in machining processes where the parameter space is intricate and the relationships between parameters are complex.

Machine learning approaches used in this thesis are Gaussian Process Regression (GPR) with Bayesian optimization (BO) and Gradient Boosting (LS-Boost) only for tool life, that have proven effective in finding optimal solutions by exploring and exploiting the parameter space. Polynomial regression can provide an explicit formulation for regression model to express non-linear relationships between input parameters and output performance, providing a flexible framework for predicting machining outcomes that is a compulsory requirement for some optimization methods. On the other hand, Bayesian optimization offers a non-parametric and probabilistic approach to optimization, balancing exploration and exploitation to efficiently search for the global optimum in complex parameter spaces.

The final contribution of this study is its inclusivity for the whole process. Recent studies generally focus on a specific parameter such as only tool life extension or form error minimization. These can contain energy consumptions [10] or cost functions [11]. Many other evolutionary techniques, such as Teaching-Learning-Based Optimization, multi-objective optimization, simulation-based models, and bio-inspired algorithms have been reviewed [12]. These methods offer robust solutions for optimizing machining parameters, balancing multiple objectives, and addressing the complexities of modern manufacturing environments. This study aims to fulfill the lifespan of manufacturing process with diverse outputs to control.

1.2 Problem Definition

In this study, a ML-based optimization technique was employed to optimize the machining parameters for a chatter-free milling operation with maximum productivity. Productivity was defined as a multi-objective function encompassing the maximization of material removal rate, tool life, and minimization of power consumption. A high material removal rate combined with a long tool life and low power consumption can significantly reduce production costs and enhance the output of machining operations. For the finishing process, form error was also considered as one of the objective functions due to its considerable effect on surface roughness. The cutting forces used for form error and power consumption calculation were estimated using a physics-based ML model. According to the obtained results, Bayesian optimization with Gaussian Process Regression offered a robust framework for efficiently optimizing the objective functions, while effectively suppressing chatter. Chatter not only deteriorates surface quality but also reduces tool life and increases production costs. By leveraging a probabilistic model to guide the search process, Bayesian optimization balances exploration and exploitation, enabling the discovery of optimal solutions with fewer evaluations compared to traditional optimization methods such as genetic algorithm and particle swarm optimization. Furthermore, the study demonstrated that machine learning-based optimization techniques could provide a more adaptive and intelligent approach to milling parameter optimization. The ability to incorporate multiple objectives and constraints into the optimization process allowed for a more comprehensive and practical solution to real-world machining challenges. This approach not only enhanced productivity but also improved the overall quality and efficiency of the milling operations. Finally, a specialized software application was developed to enhance the optimization of machining parameters.

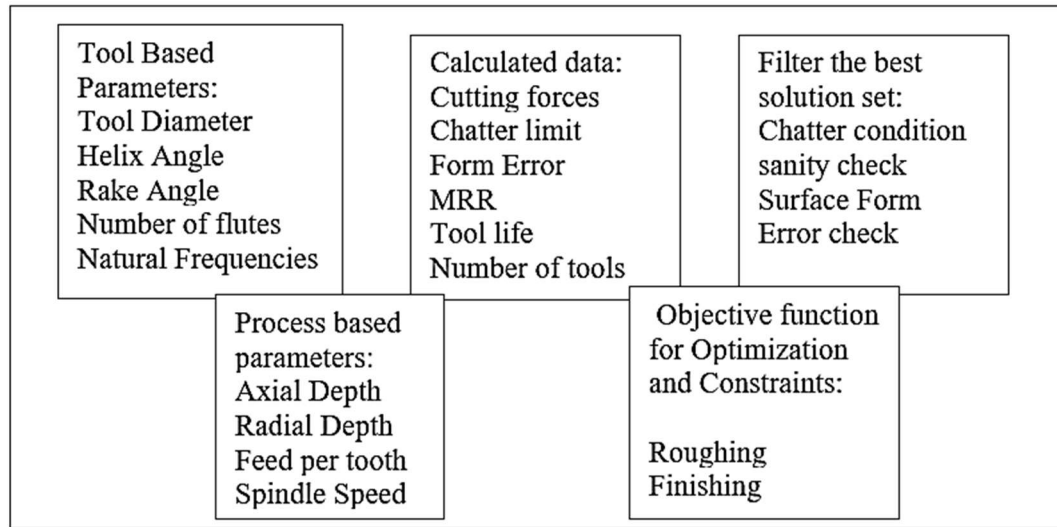


Figure 1. Overall ML process schematic representation

1.3 Methodology

The objective of this thesis is to compute an optimization function for the selection of optimum cutting parameters as axial depth of cut, radial depth of cut, feed rate and spindle speed. Machine learning process requires input data for further prediction, hence a dataset including cutting forces, MRR values, form error and tool life calculations has been prepared for 24000 different scenarios.

Variables to optimize	Outputs for Objective Function
$X_1 \rightarrow n = \text{number of flutes}$	$Y_1 \rightarrow \text{Material Removal Rate}$
$X_2 \rightarrow a = \text{axial depth of cut}$	$Y_2 \rightarrow \text{Tool Life}$
$X_3 \rightarrow b = \text{radial depth of cut}$	$Y_3 \rightarrow \text{Form Error}$
$X_4 \rightarrow N = \text{spindle speed}$	$Y_4 \rightarrow \text{Power Consumption}$
$X_5 \rightarrow f_t = \text{feed rate}$	$Y_5 \rightarrow \text{Torque}$
	$Y_6 \rightarrow \text{Tool Bending Stress}$

Table 2. Variable list of optimization problem

Following the data preparation step, Gaussian Process regression algorithm has been compiled to formulate cutting forces and the output parameters. Normalizing the data is critical since the scales are different than each other. For roughing operation, maximizing Y_1 and Y_2 has been calculated with Bayesian Optimization algorithm. Best 20 solutions have been filtered regarding the chatter condition. A similar approach has been repeated for finishing operation: the same objective function has been repeated to achieve only the form error constraint and chatter condition is not risk for this case unless the depths are increased significantly. The constraint for the form error is identified by the tolerance band. The weight of each hyperparameter has been verified by a sensitivity check and a GUI was developed for user friendly experience.

2. Data Preparation for Machine Learning

In this section, the detailed methodology employed for optimizing machining process parameters through machine learning is presented. This approach relies on Bayesian Optimization, a powerful probabilistic model-based optimization algorithm that excels in managing complex, high-dimensional search spaces where multiple interacting parameters are present [13,14]. Figure 2 provides a detailed illustration of the methodology employed in the proposed ML-based optimization.

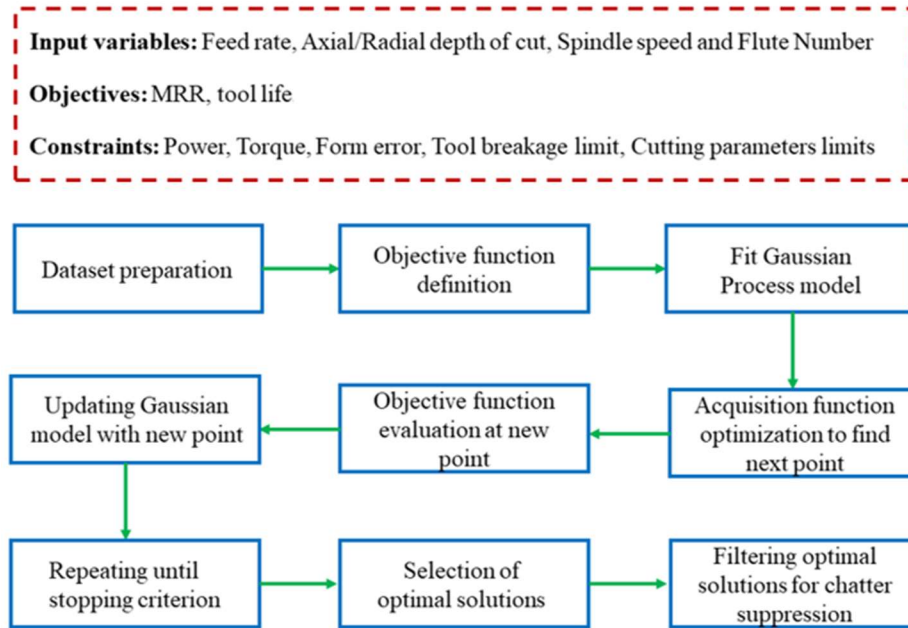


Figure 2. f Flowchart of ML-based optimization for milling with maximum productivity

The optimization process begins with the preparation of a dataset comprising input parameters and their corresponding outputs. This data contains force calculation, maximum material removal (MRR), chatter condition, form error values, tool life and tool bending stress calculations based on different cutting scenarios. The list of varying inputs is mainly divided into two categories: tool geometry related parameters and process related parameters. Tool related parameters contain tool diameter, helix angle, rake angle, and number of flutes. Only flute number has been considered as optimization variable, whereas the other tool

related parameters have been assumed as constant. Tool diameter, helix angle and rake angle are 16mm, 30° and 5° respectively. Process related parameters are spindle speed, feed per tooth, axial and radial depths, all of them are optimization variables. All calculations have been performed on milling operation of Titanium Alloy (Ti-6Al-4V) with carbide tool.

2.1 Cutting Forces

Cutting forces are always a major concern of the milling process and different modeling approaches are available such as analytical, numeric or mechanistic modeling. Since cutting force models contain some assumptions and some of them cannot be measured or observed in detail due to technological limitations, generally these models are combined with an amount of testing effort.

Cutting force calculations begin with a deep understanding of orthogonal cutting model proposed by Merchant [15], which provides an equation for shear angle by using minimum energy principle. This equation assumes that of that shear zone is a thin plane. Another shear angle calculation by Krystof based on maximum shear stress principle assumes that shearing of the workpiece coincides with the maximum shear stress direction. [16] Successively, Lee and Shaffer [17] and Palmer and Oxley [18] used a thick zone model to calculate shear angle by implementing the law of plasticity.

Armarego and Brown [19] conducted an in-depth study on the mechanics of oblique cutting and extended the principles of orthogonal cutting to establish relationships between cutting parameters such as shear angle, shear stress, and friction coefficient. Additionally, Altintas [20] proposed a practical method to predict oblique cutting forces using orthogonal cutting tests. This approach is a highly accurate way to model the oblique cutting process by applying oblique transformations to orthogonal data. Conversely, Stabler [21] examined the geometry of oblique cutting and introduced a widely accepted chip flow law, which assumes that the chip flow angle is equal to the angle of obliquity. However, this law does not account for the

effects of tool geometry, friction, and shear angle, potentially leading to significant errors in predicting cutting force coefficients under various cutting conditions. In addition to these approaches, more recent models have also been developed such as thermo-mechanical model by Budak and Ozlu [22], FEM based model by Jin and Altintas [23] and a hybrid approach encountering machine learning [24].

Because orthogonal cutting database is more effective method with respect to mechanistical method due to lower testing requirements and the database on both shear parameters and edge coefficients is available in CutPro software developed by Altintas [25], cutting forces were calculated by using shear angle, shear stress and friction coefficients.

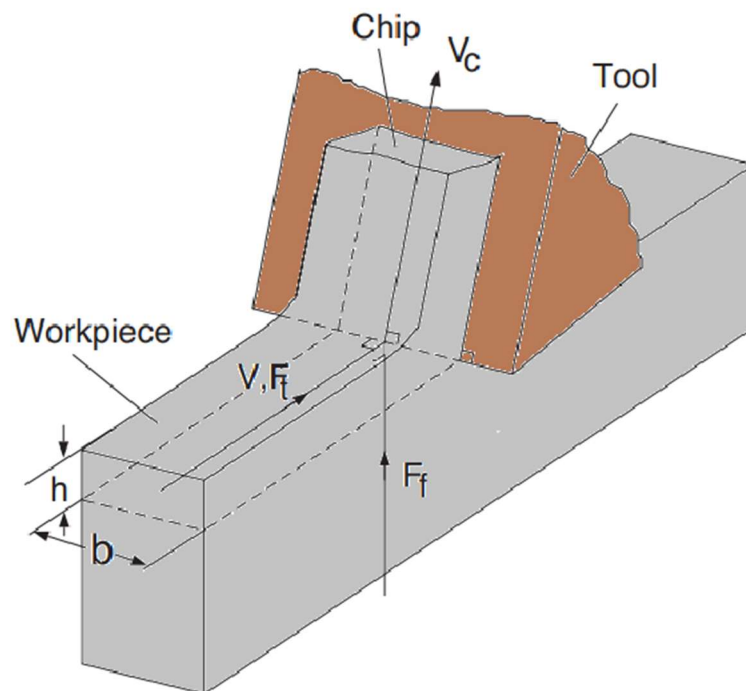


Figure 3. The representation orthogonal cutting geometry

The pseudocode for the simulation of milling cutting forces is shown as below:

Inputs:

- (a) Tool geometry related parameters:
tool diameter, helix angle, rake angle, flute number and rake angle
- (b) Process related parameters:
Spindle speed, feed rate, axial/radial depth of cut and milling mode as up/down milling
- (c) Orthogonal database related to workpiece/tool pair:
Shear angle, shear stress, friction angle and edge force coefficients (K_{te} , K_{re} and K_{ae})
- (d) Simulation related parameters:
Increment for angular integration and increment for axial integration

Calculation set 1:

- (a) Start and exit angles:

- a. Up milling:

$$\phi_s = \cos^{-1} \left(1 - \frac{2a}{D} \right)$$

$$\phi_e = 0$$

- b. Down milling

$$\phi_s = 0$$

$$\phi_e = \cos^{-1} \left(1 - \frac{2a}{D} \right)$$

(2.1)

- (b) Specific cutting force coefficients: K_{tc} , K_{rc} and K_{ac}

$$\begin{aligned}
\text{a. } K_{tc} &= \frac{\tau_s \cos(\beta_n - \alpha_n) + \tan i \tan \eta \sin \phi_n}{\sin \phi_n \sqrt{\cos^2(\phi_n + \beta_n - \alpha_n) + \tan^2 \eta \sin^2 \beta_n}}, \\
\text{b. } K_{fc} &= \frac{\tau_s \sin(\beta_n - \alpha_n)}{\sin \phi_n \cos i \sqrt{\cos^2(\phi_n + \beta_n - \alpha_n) + \tan^2 \eta \sin^2 \beta_n}}, \\
\text{c. } K_{rc} &= \frac{\tau_s \cos(\beta_n - \alpha_n) \tan i - \tan \eta \sin \phi_n}{\sin \phi_n \sqrt{\cos^2(\phi_n + \beta_n - \alpha_n) + \tan^2 \eta \sin^2 \beta_n}}.
\end{aligned} \tag{2.2}$$

$$\text{(c) Instantaneous Chip thickness: } h = f \cdot \sin(\theta) \tag{2.3}$$

Calculation Set 2:

(a) Incremental force calculation to obtain tangential, radial and axial forces by

- a. Integrating one spindle rotation
- b. Integration for the total number of cutting edges
- c. Integration for the axial disks

(b) Summation of the forces

$$\begin{aligned}
\text{a. } F_t &= \sum_{i=1}^N \sum_{\theta=0}^{360} (K_{tc} \cdot h + K_{te}) \cdot dz \\
\text{b. } F_r &= \sum_{i=1}^N \sum_{\theta=0}^{360} (K_{rc} \cdot h + K_{re}) \cdot dz \\
\text{c. } F_a &= \sum_{i=1}^N \sum_{\theta=0}^{360} (K_{ac} \cdot h + K_{ae}) \cdot dz
\end{aligned} \tag{2.4}$$

Outputs:

- (a) Simulated F_t , F_r and F_a forces (tangential, radial and axial forces)
- (b) Simulated F_x , F_y and F_a forces (feed, normal and axial forces)
- (c) Power and torque requirements of the process

$$\begin{aligned}
\text{Power} &= F_t V_c \\
\text{Torque} &= F_t R
\end{aligned} \tag{2.5}$$

2.2 Form Error

For the finishing processes, the form error was also considered in the optimization problem, due to its strong correlation with surface roughness. Form error is dependent on tool and workpiece deflection, as explained by equation (6):

$$e(x, y) = \delta_y(z) - y_p(x, y) \quad (2.6)$$

where, where $\delta_y(z)$ is the tool deflection at an axial position z , and $y_p(x, z)$ is the work deflection at the position (x, z) . In this study, the workpiece deflection wasn't itself included in the objective function, since, by minimizing tool deflection, form error is also minimized and there is no need to include workpiece deflection in the objective function. To calculate the tool deflection, first, the surface generation points must be determined. These points are the intersections of the helical flutes with the workpiece surface, satisfying the immersion conditions necessary for surface generation [26,27], as explained by equation (7):

$$\phi_j = \phi + j\phi_p - \frac{\tan\beta}{R} z = \begin{cases} 0, & \text{for up milling} \\ \pi, & \text{for down milling} \end{cases} \quad (2.7)$$

where, R is the tool radius, $\phi_j(z)$ is the immersion angle for flute j at axial depth of z , ϕ_p is the cutter pitch angle, and β is the helix angle. Consequently, the axial coordinate of the flute/surface contact point in axial direction is determined:

$$Z_j(\phi) = \begin{cases} \frac{R(\phi + j\phi_p)}{\tan\beta}; & \text{for up milling} \\ \frac{R(\phi + j\phi_p - \pi)}{\tan\beta}; & \text{for down milling} \end{cases} \quad (2.8)$$

Using cantilever beam theory, the tool deflection at surface generation points can be calculated by equation (9) [15]:

$$\begin{aligned}\delta_y(k, m) &= \frac{\Delta F_{km} z_m^2}{6EI} (3v_m - v_k) + \frac{\Delta F_{km}}{k_x}; & 0 < v_k < v_m \\ \delta_y(k, m) &= \frac{\Delta F_{km} z_m^2}{6EI} (3v_k - v_m) + \frac{\Delta F_{km}}{k_x}; & v_m < v_k \\ \delta_y(k) &= \sum_{m=1}^n \delta_y(k, m)\end{aligned}\quad (2.9)$$

where, E is the Young's modulus, L is the gauge length of the cutter, I is the area moment of inertia, n is the number of elements along the axial direction, $v_k = L - z_k$, and F_m is the normal force at the m^{th} element, which is calculated using a physics-based ML model [24], similar to the approach used for power/torque calculation. k_x is the linear clamping stiffness at the tool-holder interface, equal to 19.8 kN/mm for a carbide end mill with 19 mm diameter and 55.6 mm gauge length [26]. To calculate the moment of inertia of the cutting tool, the inertia of each region of the tool's cross-section is determined analytically, starting with the first region and then transforming and summing the contributions from other regions, as illustrated in Figure 4. The inertia of region 1 is obtained by calculating the equivalent radius (R_{eq}) based on the arc's radius (r) and the position of its center (a), as explained by equation (2.10). Then, the total moment of inertia is computed by summing the moments from all regions and adding the effect of the arcs due to flute depths as stated in equation (2.11) [26,27].

$$\begin{aligned}R_{\text{eq},4\text{-flute}}(\theta) &= a \sin(\theta) + \sqrt{(r^2 - a^2) + a^2 \sin^2(\theta)}; & 0 < \theta \leq \frac{\pi}{2} \\ R_{\text{eq},3\text{-flute}}(\theta) &= a \cos\left(\theta + \frac{\pi}{3}\right) + \sqrt{(r^2 - a^2) + a^2 \cos^2\left(\theta + \frac{\pi}{3}\right)}; & 0 < \theta \leq \frac{2\pi}{3} \\ R_{\text{eq},2\text{-flute}}(\theta) &= -a \cos(\theta) + \sqrt{(r^2 - a^2) + a^2 \cos^2(\theta)}; & 0 < \theta \leq \pi\end{aligned}\quad (2.10)$$

$$I_{xx,4\text{-flute}} = -\frac{1}{8}\pi\left(\frac{f_d}{2}\right)^4 + \frac{\pi}{2}\left(\frac{f_d}{2}\right)^2\left(r + a - \frac{f_d}{2}\right)^2 + \int_0^{\frac{\pi}{2}} \int_0^{R_{\text{eq},4\text{-flute}}(\theta)} \rho^3 \sin^2(\theta) d\rho d\theta \quad (2.11)$$

$$I_{yy,4\text{-flute}} = -\frac{1}{8}\pi\left(\frac{f_d}{2}\right)^4 + \int_0^{\frac{\pi}{2}} \int_0^{R_{\text{eq},4\text{-flute}}(\theta)} \rho^3 \cos^2(\theta) d\rho d\theta$$

The same approach is also applicable to the 3-flute and 2-flute tools. After performing the necessary transformations, the moments of inertia are calculated by equation (2.12) [27]:

$$\begin{aligned} I_{xx,4\text{-flute};\text{TOTAL}} &= I_{yy,4\text{-flute};\text{TOTAL}} = 2(I_{xx,4\text{-flute}} + I_{yy,4\text{-flute}}) \\ I_{xx,3\text{-flute};\text{TOTAL}} &= I_{yy,3\text{-flute};\text{TOTAL}} = 1.5(I_{xx,3\text{-flute}} + I_{yy,3\text{-flute}}) \\ I_{xx,2\text{-flute};\text{TOTAL}} &= 2(I_{xx,2\text{-flute}}); \quad I_{yy,2\text{-flute};\text{TOTAL}} = 2(I_{yy,2\text{-flute}}) \end{aligned} \quad (2.12)$$

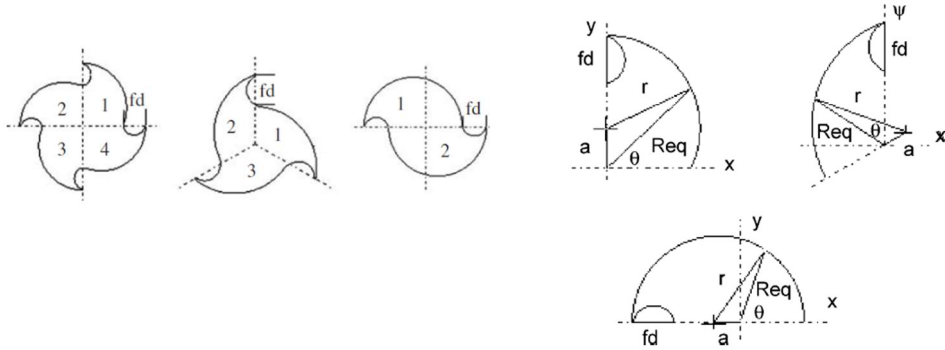


Figure 4. Cross section of 2, 3 and 4-flute end mills [15].

2.3 Tool Life

Cutting tools can be used until cutting edge quality is lost because of wear or breakage. When a tool loses its sharpness, the dimensional accuracy is adversely affected, and the tool needs to be replaced. The most economical machining time is dependent on the tolerances of the part and wear rate of the tool. Wear is mainly dependent on cutting speed since higher cutting speeds increase the temperature between tool and workpiece exponentially. However, milling process is complex process where the cutting edge periodically enters and exits to the workpiece. This intermittent structure causes cyclic stress and temperature variation during the process.

Regarding roughing and finishing operations, the approaches about tool life changes. For roughing operations, changing the tool during the cutting process may not cause a problem since any mark on the surface will be removed with the following pass. However, it is of great importance to complete finishing operation with one tool since any mismatch mark may result in the rejection of the part depending on the design function of the feature.

For the calculation of the tool wear, Taylor's equation is used.

$$V_c T^n f_z^m = C \quad (2.13)$$

Lee and Yoon [28] have studied tool life modeling with power consumption using Taylor's equation and developed a direct tool life model, the experimental verification of this study is conducted with Titanium alloy and uncoated solid carbide four-flute plain end mill with a diameter of 12 mm. The other parameters of the tools are as follows: helix angle 30°, total tool length is 83 mm, and cutting-edge length is 25 mm. (TSE-4120M-TT5515; Taegutec Ltd., Korea). This study contains an adequate number test conducted with different cutting

parameters and the constant parameters of Taylor's equation was obtained by fitting experimental results to the equation (2.13). Here, V_c represents cutting speed, f_z represents feed per tooth, and T represents the tool life, where n , m , and C are constants.

($n = 0.2428$, $m = 0.890$, $C = 8.4864$)

2.4 Material Removal Rate (MRR)

Material removal rate (MRR) is found by multiplying the process cutting parameters: axial depth of cut, radial depth of cut and feed rate as mm/min. The unit of this parameter is mm^3/min . [29]

$$\text{Material removal rate} = a * b * f_{\text{tooth}} * N * n \quad (2.14)$$

2.5 Tool Bending Stress

The tool breakage limit is estimated based on the Euler-Bernoulli beam theory. This estimation involves calculating the bending stress for a beam under uniform load, followed by applying Weibull analysis to a four-point bend test, as explained by equation (2.15) [30].

$$\sigma_{\text{max-cutte}} = 1.25 \left(\frac{87.63}{H}\right)^{1/m} \left(\frac{9.53}{R_s}\right)^{2/m} \sigma_{\text{max-bendin}} \quad (2.15)$$

where, H is the flute length, R_s is the shank radius, and m refers to Weibull modulus. The tool breakage limit necessitates that the maximum stress in the cutting tool must not exceed the mean failure stress of the carbide end mill, which is 1533 MPa [27].

2.6 Power and Torque Consumption

Power and torque values are the parameters that will be limited by the machining center in the optimization process. In this step of the study, these values are calculated by using the mechanistic force model where, V_c is the cutting speed, f is feed rate per tooth, n is spindle speed, N is the number of teeth, V_f is the feed velocity ($= f * N * n$), R is the tool radius, F_t is the tangential force and F_f is the feed force. During optimization step, this mechanistic force calculation will be replaced by the physics-based M model which performs new predictions based on the regression function.

$$\begin{aligned} Power &= F_t V_c \\ Torque &= F_t R \end{aligned} \tag{2.16}$$

2.7 Limits for Data Preparation

Data preparation is the input for machine learning process, hence wider definitions will be helpful for the regression to perform better. The upper and lower limits of the cutting parameters were determined according to the machine tool limits and the tool manufacturer's data to establish a feasible solution set and save computational time.

$$\left\{ \begin{array}{l} 0.5 \leq \text{axial depth of cut} \leq 20 \text{ mm} \\ 10\% d_{\text{tool}} \leq \text{radial depth of cut} \leq 100\% d_{\text{tool}} \\ 0.3 * R_{\text{hone}} \leq \text{feed rate} \leq 0.15 \text{ mm/tooth} \\ 1000 \leq \text{spindle speed} \leq 10000 \text{ rpm} \\ 2 \leq \text{tooth number} \leq 4 \end{array} \right\}$$

3. Machine Learning Model: GPR with Bayesian Optimization

3.1 GPR and BO for all output variables

This section explains Gaussian Process Regression (GPR), and its integration with Bayesian optimization (BO) theory. Bayesian optimization utilizes a more strategic approach where it employs a probabilistic model to guide the optimization process, making informed decisions about where to sample next based on prior evaluations and predictions about the objective function's behavior. This iterative process involves exploring new possibilities and exploiting known high-value areas until an optimal solution is found or a stopping criterion is met [32]. The primary advantage of Bayesian optimization is its ability to efficiently handle expensive functions (considering both computational time and memory), achieving effective optimization outcomes with fewer evaluations. The key components of the Bayesian optimization framework include the surrogate model, acquisition function, and optimization loop, as described in the following subsections.

A key component of Bayesian optimization is the surrogate model, which approximates the objective function. This model serves as a probabilistic approximation of the true, often expensive-to-evaluate objective function. By using the surrogate model, Bayesian optimization can explore the search space more efficiently and make informed decisions about where to sample next. In the context of Bayesian optimization, the Gaussian Process Regression (GPR) is commonly employed as the surrogate model due to its flexibility and efficacy in capturing complex functions.

Once the data preparation step has been completed, the selection of the most suitable machine learning algorithm step started. Regarding the calculation of the output parameters to be used for both new data generation before optimization step, GPR model was selected. GPR is a non-linear regression method which is distinguished with its ability for high dimensional data and complex interactions. The “*fitrgp*” function is used to fit a Gaussian

Process Regression model. The kernel function is set to squared exponential, which is commonly used for GPR. For each output variable, predictions are made, and metrics such as Mean Squared Error (MSE) and R-squared (R^2) are calculated as listed in Table 4. The results are printed, and a scatter plot of actual vs. predicted values is generated.

Hyperparameter	Description	Possible Values
Basis Function	The basis function for the Gaussian process.	'none', 'constant', 'linear', 'pure quadratic'
Kernel Function	The kernel (covariance) function for the Gaussian process.	'Squared exponential', 'matern32', 'matern52', 'rational quadratic', 'exponential', 'ardmatern52', 'ard exponential'
Sigma	The noise level to add to the diagonal of the covariance matrix.	Any positive real number (e.g., 1e-3, 1e-4)
Optimizer	The optimization algorithm used to minimize the negative log marginal likelihood.	'fminunc', 'quasi-newton', 'lbfgs'

Table 3. Hyperparameters of Bayesian Optimization and Gaussian Process Regression

	Summary of Metrics
Mean Square Error (MSE)	The average of the squares of errors (difference between predicted and actual values).
Root Mean Square Error (RMSE)	The square root of the MSE, giving a measure of error in the same units as the output variable.
R-Squared (R^2)	The proportion of variance in the dependent variable that can be explained by the independent variables.

Table 4: Summary of ML performance metrics

The Bayesian optimization process involves iterating between sampling new points and updating the surrogate model. The steps are as follows:

Initialize Samples: Select initial points to evaluate the objective function.

Fit GPR Model: Build the GP model using the initial data.

Define Acquisition Function: Choose an acquisition function to guide the search for the next sampling.

Optimize Acquisition Function: Find the point that maximizes the acquisition function.

Evaluate Objective Function: Compute the actual objective function value at the new point.

Update GPR Model: Update the model with the new data.

Repeat: Continue the process until a stopping criterion is met.

GPR provides a robust and probabilistic framework for modeling the objective function, making it a popular choice in optimization tasks where evaluations are costly. A Gaussian Process is defined as a collection of random variables, any finite number of which have a joint Gaussian distribution. It is characterized by a mean function and a covariance function (also known as the kernel), which together encode assumptions about the smoothness, continuity, and overall behavior of the objective function. The mean function represents the expected value of the objective function at any point in the input space, while the covariance function describes how values of the function at different points are related to each other [33]. However, GPR has one critical limitation: it does not produce a closed-form regression formula like polynomial regression. Instead, it models a distribution over possible functions based on the training data and the specified kernel.

GPR not only provides a prediction of the objective function's value but also quantifies the uncertainty associated with these predictions. This uncertainty estimation is fundamental to the Bayesian optimization process, guiding the selection of new candidate solutions by balancing exploration of uncertain regions with exploitation of known good regions.

Overall, the surrogate model in optimization, and specifically GPR, plays a critical role in efficiently navigating the search space and converging to optimal solutions by leveraging probabilistic reasoning and adaptive sampling strategies.

Let $f(x)$ represent the objective function targeted for optimization, which can be modeled as a Gaussian Process with mean function $\mu(x)$ and covariance function $k(x,x')$:

$$f(x) \sim \mathcal{GP}(\mu(x), k(x, x')) \quad (3.1)$$

where the mean function $\mu(x)$ represents the expected value of $f(x)$ and the covariance function $k(x,x')$ describes the correlation between function values at different inputs, as explained by equation (3.2).

$$\begin{aligned} \mu(x) &= E[f(x)] \\ k(x, x') &= E[(f(x) - \mu(x))(f(x') - \mu(x')))] \\ f(x_*) \mid X, Y, x_* &\sim \mathcal{N}(\mu_*(x_*), \sigma_*^2(x_*)) \end{aligned} \quad (3.2)$$

where the posterior mean and variance are given by equation (3.3):

$$\begin{aligned} \mu_*(x_*) &= k(x_*, X)[K(X, X) + \sigma^2 I]^{-1} Y \\ \sigma_*^2(x_*) &= k(x_*, x_*) - k(x_*, X)[K(X, X) + \sigma^2 I]^{-1} k(X, x_*) \end{aligned} \quad (3.3)$$

Here, $k(x,x)$ is the covariance matrix computed from the training data, $k(x^*,x)$ is the covariance vector between the new point and the training points [33].

3.2 Acquisition Function

The acquisition function guides the selection of the next sampling point based on the surrogate model's predictions. It quantifies the trade-off between exploration (sampling in regions with high uncertainty) and exploitation (sampling in regions with high predicted performance). Common acquisition functions include:

Expected Improvement (EI):

$$EI(x) = E[\max(f(x^+) - f(x), 0)] \quad (3.4)$$

where $f(x^+)$ is the best observed value so far.

Probability of Improvement (PI):

$$PI(x) = \Phi\left(\frac{f(x^+) - \mu(x)}{\sigma(x)}\right) \quad (3.5)$$

where ϕ is the cumulative distribution function of the standard normal distribution.

Upper Confidence Bound (UCB):

$$UCB(x) = \mu(x) + \kappa\sigma(x) \quad (3.6)$$

where κ is a parameter that controls the balance between exploration and exploitation.

The MATLAB function used for GPR model:

```
gprModel = fitrgp(X, Y(:, i), 'KernelFunction', 'squareexponential', ...  
'OptimizeHyperparameters', 'auto', 'Verbose', 1);
```

Parameter	Description	Other Possible values
X	The matrix of predictor (input) parameters	
Y	The response (output) variable for the regression model	
Kernel Function	The function, used to define the covariance structure of the Gaussian Process. The choice of kernel affects how the model generalizes from the training data. 'squarexponential': this function assumes that points closer in the input space will have more similar outputs. It's a commonly used kernel for smooth and continuous functions, ideal for capturing the gradual trends in data.	'matern52', 'ardsquarexponential', 'rationalquadratic'
Optimize Hyperparameters	When set to 'auto', this parameter triggers automatic optimization of the kernel hyperparameters (e.g., length scale and variance) to best fit the data. This allows the model to adapt its parameters to achieve the best predictive performance. In GPR, Bayesian Optimization is selected by default among other techniques such as Grid Search, Random Search and Genetic Algorithm.	'sigma', 'basisFunction', 'KernelScale', 'Standardize', 'none'
Verbose	When Verbose is equal to '1', the function displays the optimization process details in the command window, which can be useful for tracking the optimization progress or debugging.	'0', '2', '3'

Table 5: Selected Parameters of GPR process

3.3 Model Performance

	MSE	RMSE	R^2
MRR	141689.7077	376.4169	1.0000
Tool Life	50814696919.7770	225421.1546	0.2095
Power	579.8379	24.0798	1.0000
Torque	1045.3783	32.3323	1.0000
Tool Bending Stress	63.1071	7.9440	0.9999
Form Error	0.0000	0.0017	0.9983

Table 6: GPR Model Performance Results on Output Variables

As seen in Table-4, the model performance is quite promising and has a good capability of making accurate predictions apart from Tool Life variable. R-Square value for Tool Life shows that the predictions for Tool Life will be very poor. Any optimization based on GPR prediction will mislead the optimum results.

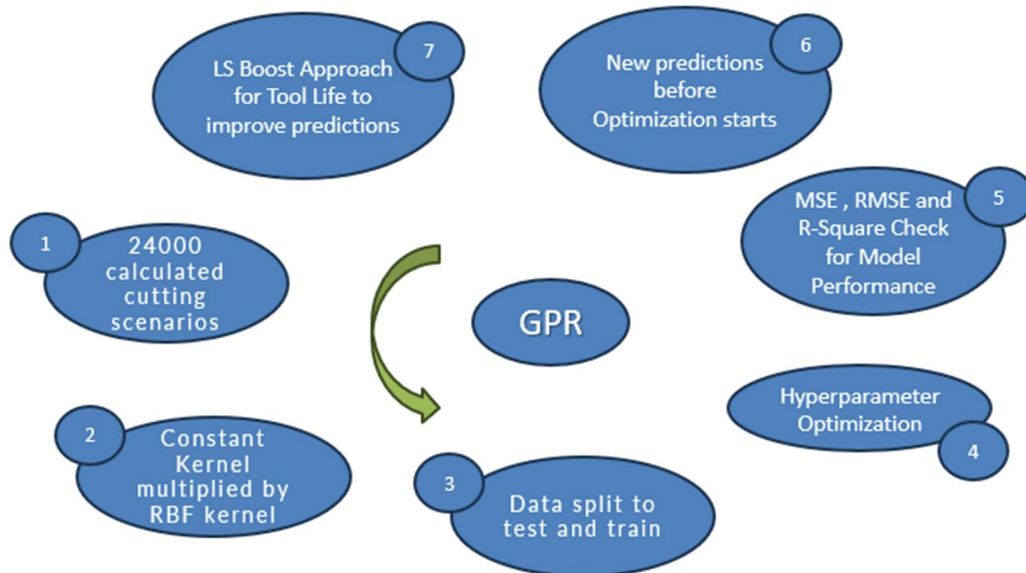


Figure 4: schematic representation of GPR

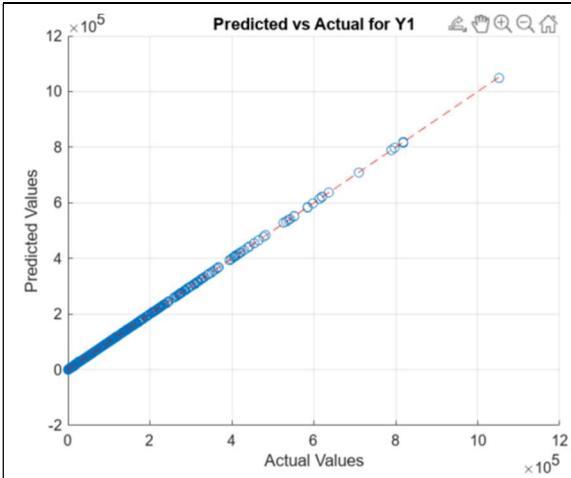


Figure 5: Comparison for MRR

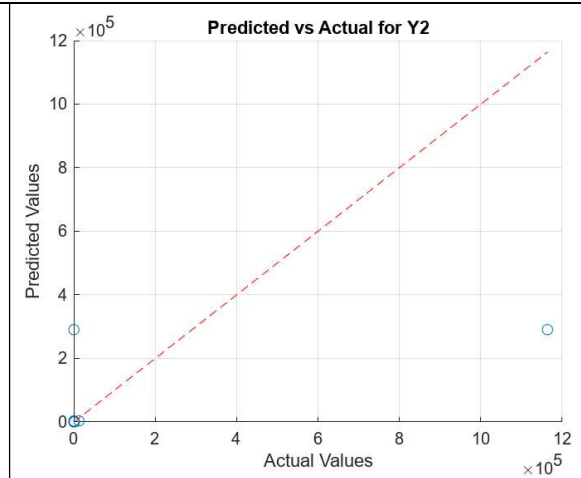


Figure 6: Comparison for Tool Life

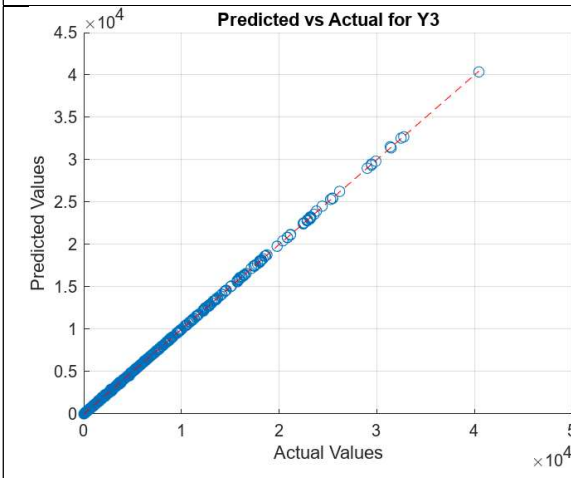


Figure 7: Comparison for Power

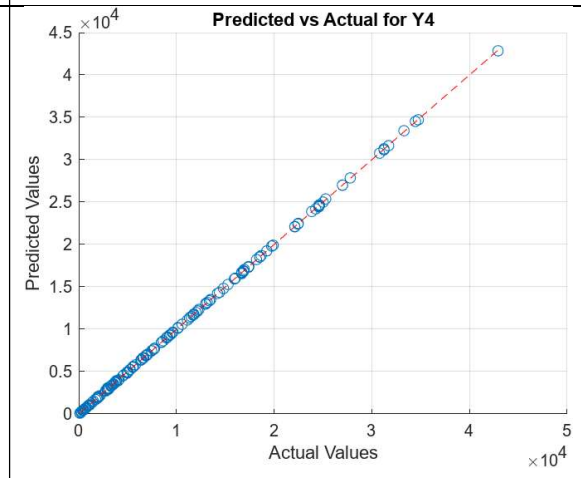


Figure 8: Comparison for Torque

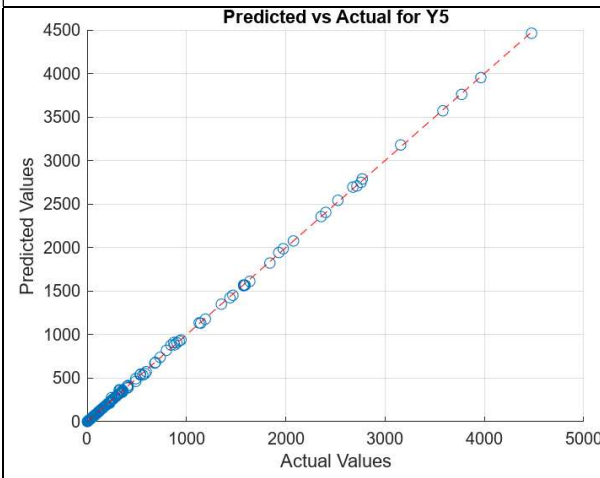


Figure 9: Comparison for Tool Bending Stress

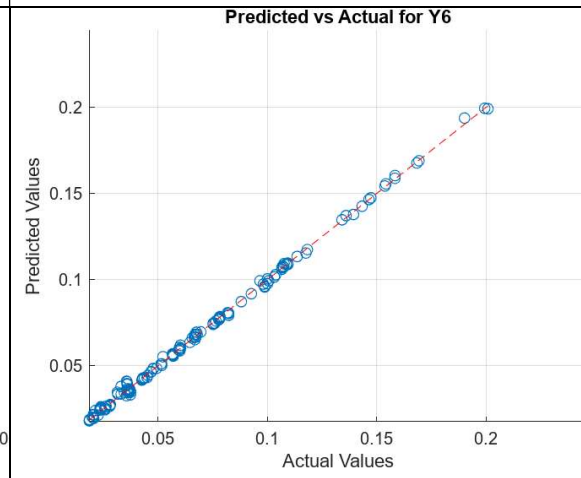
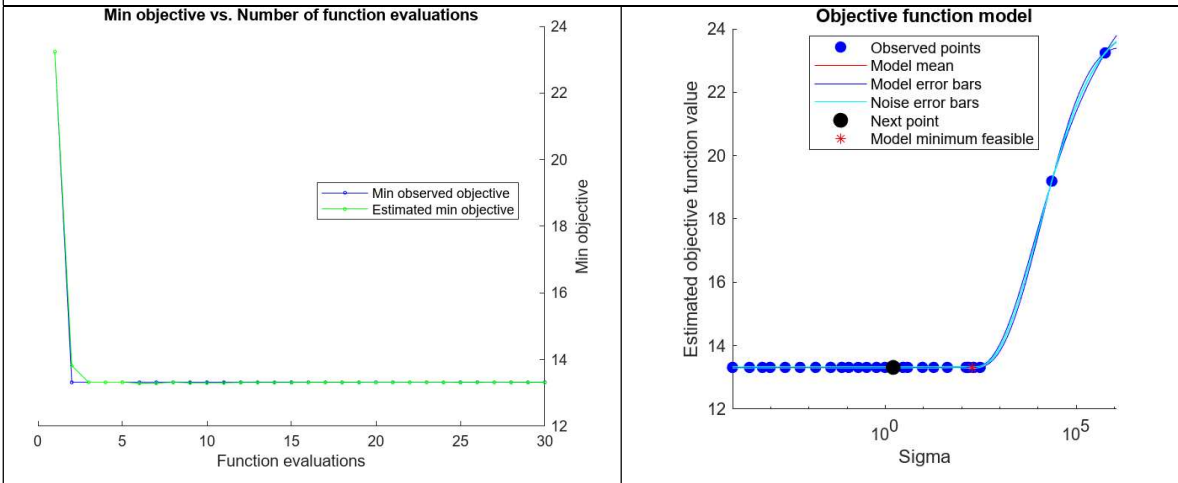


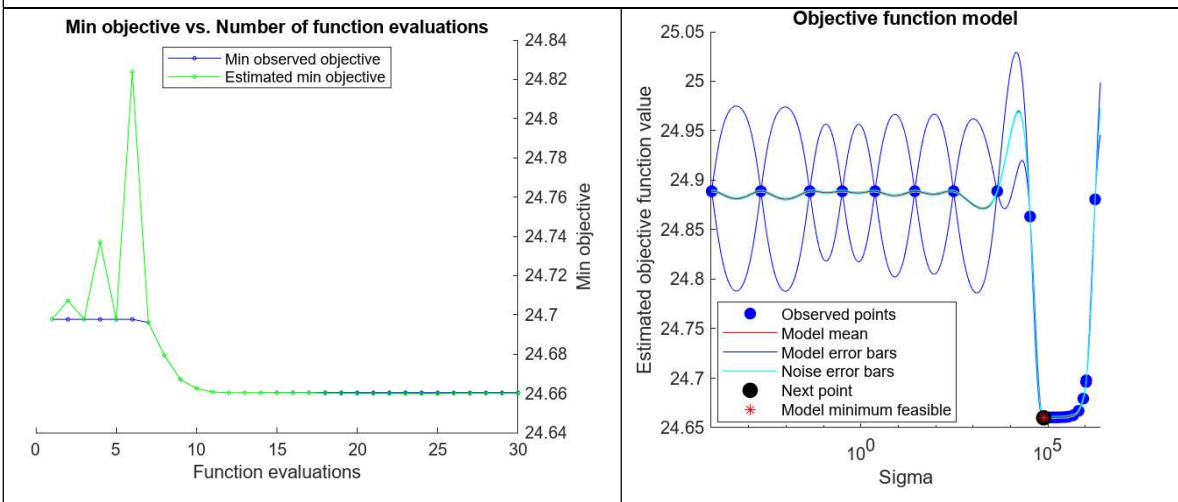
Figure 10: Comparison for Form Error

Table 7: Actual vs Predicted Plots for Output Variables

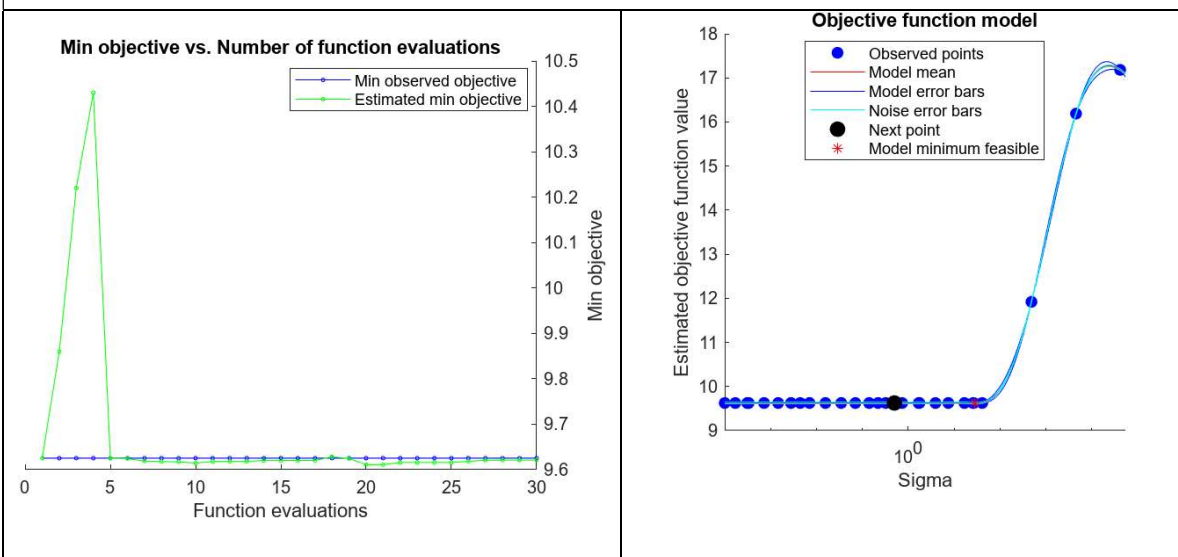
Plots for MRR



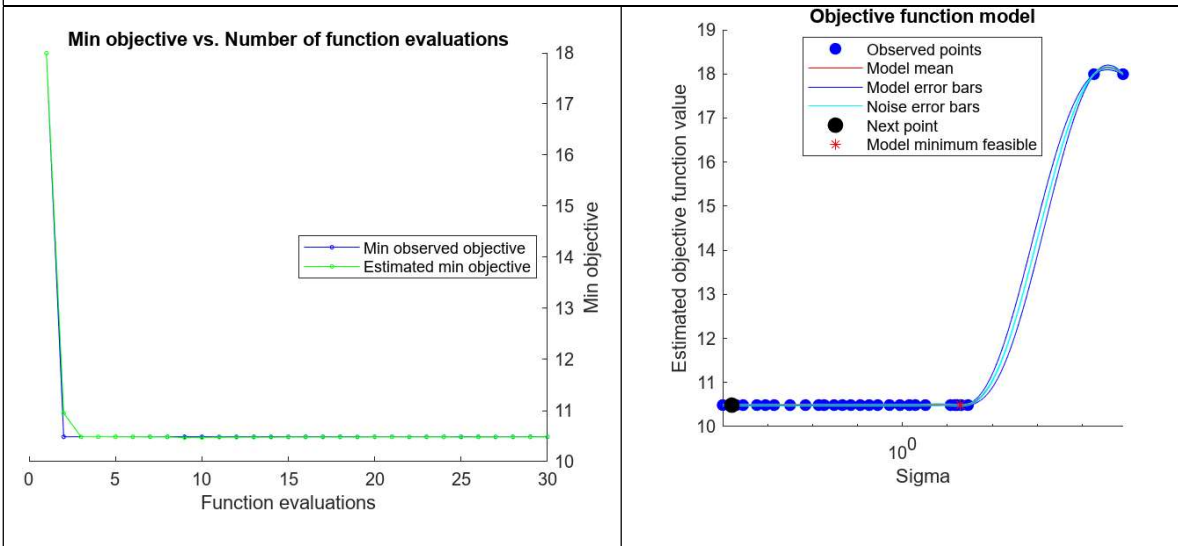
Plots For Tool Life



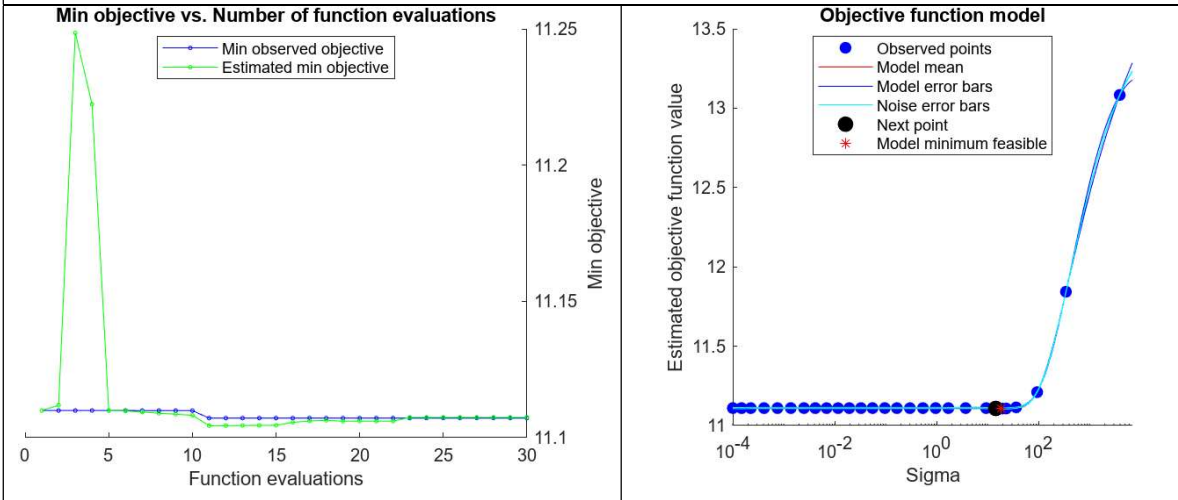
Plots for Power



Plots for Torque



Plots for Tool Bending Stress



Plots for Form Error

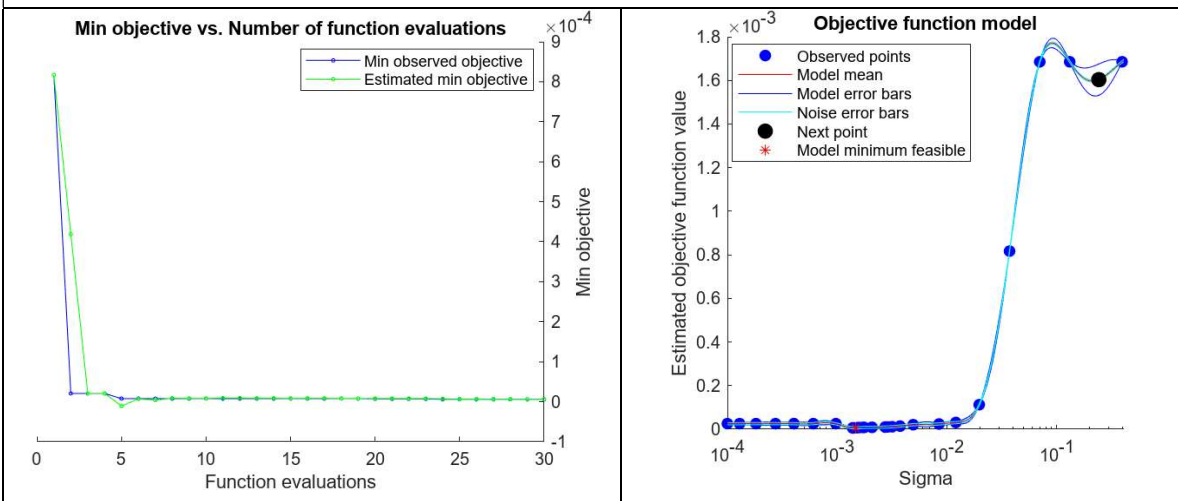


Table 8: Convergence Plots of each Output Variable

3.4 An alternative approach for Tool Life

Investigating the other regression models of machine learning approach, polynomial (as 2nd and 3rd degree of functions) and exponential models were tried as well. In addition, given that the tool life formula contains only feed rate (X_3) and cutting speed (a function of spindle speed represented as X_4), these two variables were selected as predictors rather than including all predictor variables at once. These trials ended up with $R^2 = 0.5235$ value, which is still inadequate to move into optimum parameter selection step. Furthermore, taking the logarithm of the tool life values did not help with better predictions.

LS-Boost builds a series of decision trees in sequence, with each tree correcting the errors of the previous ones. The final prediction is the weighted sum of the outputs from all individual trees. Each tree in LS-Boost focuses on minimizing the residual errors (differences between predicted and actual values) from the previous trees. This iterative correction process results in a model with higher accuracy and lower bias. Since each tree only contributes to specific regions of the input space and does not have a simple mathematical form, the ensemble does not yield a single, explicit regression equation. Instead, predictions are made by passing inputs through the series of trees and summing up their weighted outputs. To make a prediction with LS-Boost, each input is run through the ensemble, and each tree provides an output. These outputs are then combined (summed) to give the final prediction. This happens internally in the model without generating an explicit function.

Finally, LS-Boost approach ended up with a good level of predictions and a R^2 value very close to 1 as can be seen in Table-9. Actual values were compared and plotted in Figure-4. Since the results are better than expected, 4 model validation steps have been added:

1. Train-Test Split: 80% of the data used for train, 20% used for test. (cvpartition)
2. Cross-Validation: Model stability across different data splits (k-folds =5)

3. Feature Importance Check: Identify the dominant predictors
4. Visualize Residuals: Helpful to detect overfitting

As a result, all output variables have been predicted with Gaussian Process Regression apart from Tool Life which has an exponential trend. Tool Life predictions are calculated by LS-Boost approach.

	MSE	RMSE	R^2
Tool Life (Y2)	0.0000	0.0000	1.0000

Table 9: LS-Boost performance results for Tool Life

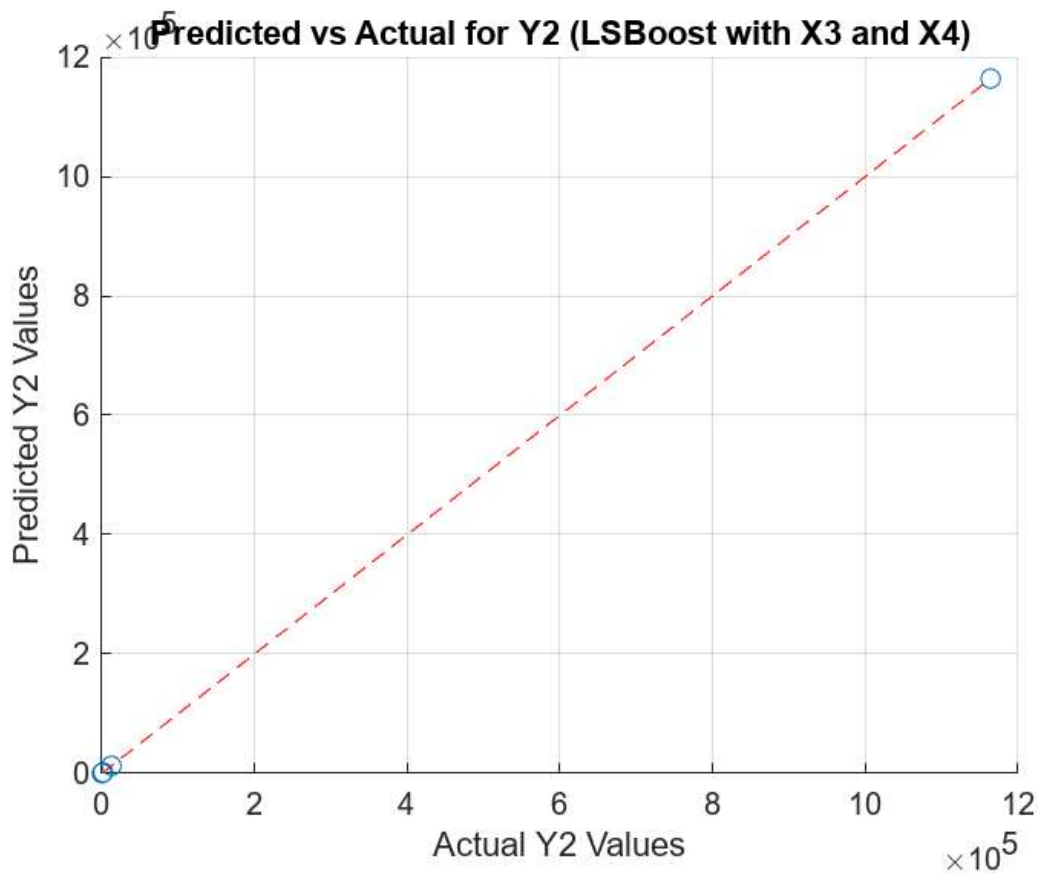
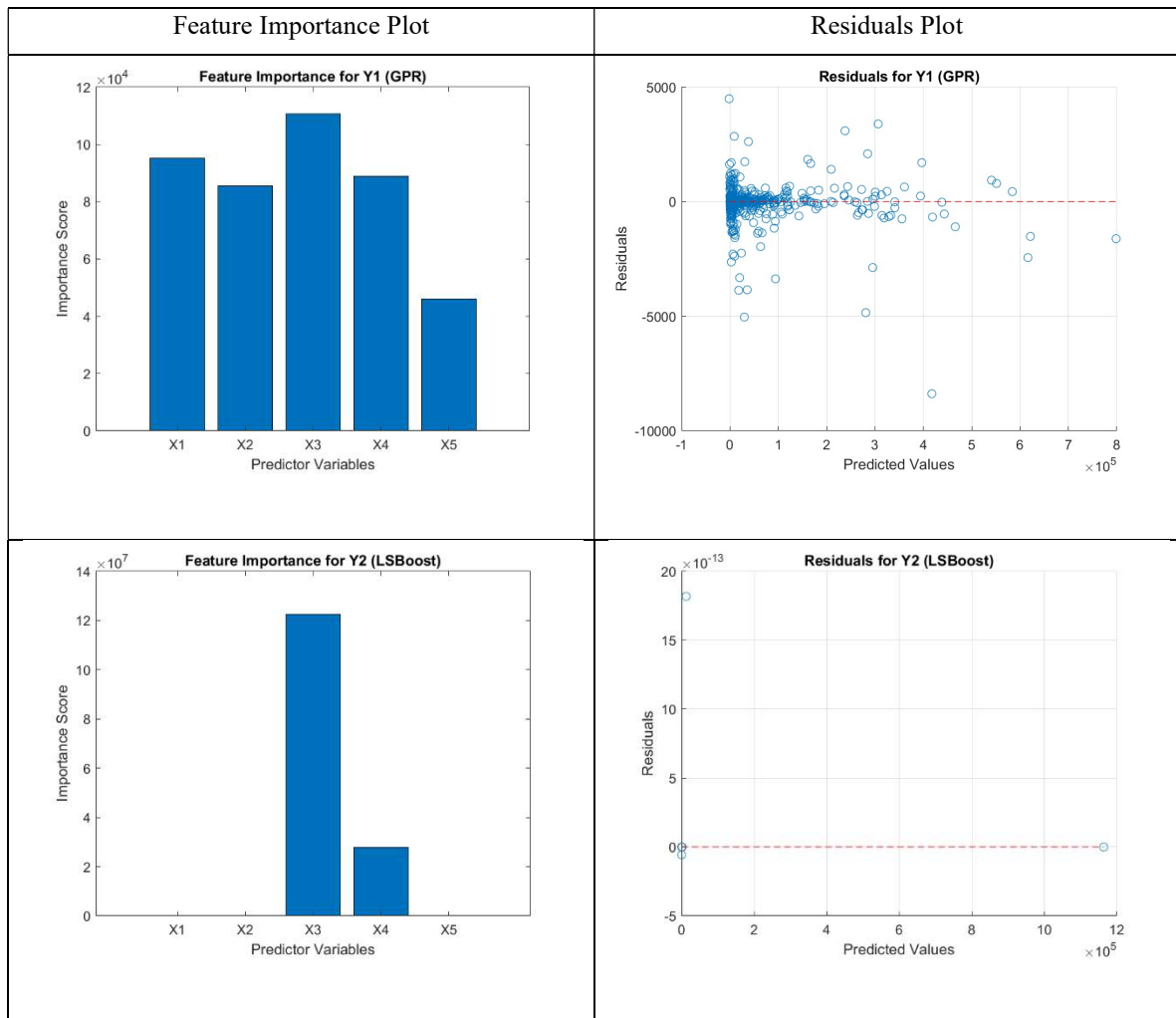
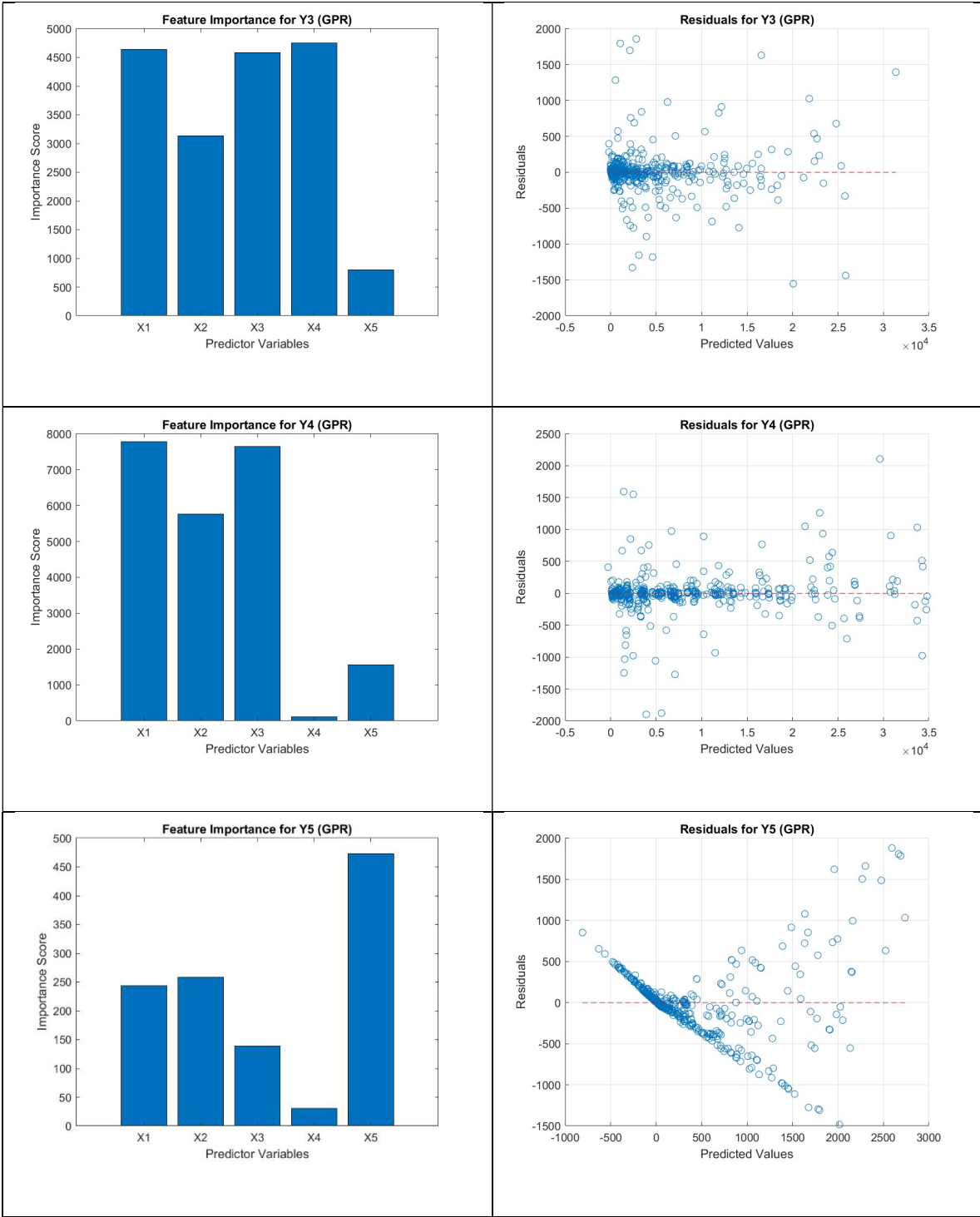


Figure 11: LS-Boost performance on Tool Life Prediction

3.5 Feature Importance and Residuals

Feature Importance reflects the idea that certain predictors (features) have more influence or impact on the model's outcomes. Residuals are named as prediction errors that indicate the discrepancy between actual and predicted values, highlighting the error in predictions.





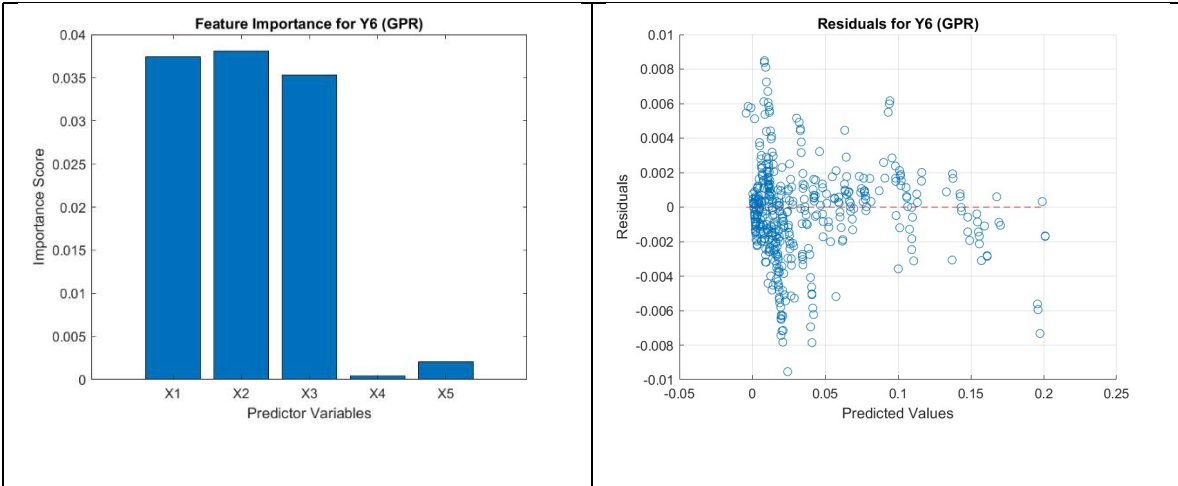


Table 10: Feature Importance and Residual Plots for each output variable

4. Optimization Method to Identify Optimum Cutting Parameters

4.1 Objective Function

The objective function for the roughing operation aims to maximize material removal rate and tool life, while suppressing chatter and satisfying tool breakage limit and power/torque restrictions. The function to be optimized is described by equation (4.1). Furthermore, the boundaries of the machine learning algorithm should be redefined with respect to tool catalog inputs for axial depth and feed per tooth or feed rate parameters.

For the finishing processes, the form error was also considered in the optimization problem as the only compulsory constraint, due to its strong correlation with surface roughness. Form error is dependent on tool and workpiece deflection, as explained by equation (4.2). Form error calculation ignores workpiece deflection, tool wear and lubricant usage at this step. The boundaries of the form error constraints directly taken from technical drawing the component. The upper can be defined by the tolerance band and lower bound can be selected as 70-80% of the upper bound. This approach avoids much better production than desired, hence decreases cost respectively. For example, if the tolerance band of the component refers to ± 0.5 mm, the boundaries as 0.4 and 0.5 mm as lower and upper bound can be selected respectively. If the part is machined with ± 0.1 mm, it means that the process still has some room to decrease cost by increasing the productivity rate.

As a unique case of production, tool life might be targeted for a minimum machining cycle. The machining operations of very large die casts like the ones to produce vehicle body components, one may prefer to define a minimum tool life to complete the entire finishing pass with only one tool and not to leave any mismatch line on surface. This type of optimization problem addresses a different solution approach. When a parameter is defined in both objective function and the constraint set, then this can be solved with non-linear constrained optimization.

maximize {Material removal rate & Tool life}; *while suppressing chatter & satisfying power/torque and tool breakage limits* (4.1)

maximize {Material removal rate & Tool life}; *while achieving design tolerance requirement so controlling form error* (4.2)

4.2 Optimization Methods and Results

In this chapter, 3 different approaches for optimization are defined in detailed: Genetic algorithm for general purpose, bayesian optimization where weight definitions are up of importance and non-linear constrained optimization for a specific condition.

Different problems require different solutions. Every solution begins with identifying a clear problem, and a well-defined problem statement makes it significantly easier to develop an effective solution. In this case, we are focused on transitioning from design concepts to producing conforming products. This shift starts with having a virtual CAD model and a technical drawing that outlines design specifications.

When a supplier receives a technical drawing along with a quotation request, one of the first considerations is the material to be machined and the required tolerance band. For instance, is the component a general-purpose automotive part with relatively broad tolerances, or an aerospace component with extremely tight tolerances? Each of these scenarios brings unique requirements.

When a large die cast for an automotive body part is considered, manufacturing such components involves producing two large dies, a process that can take days. For large surface areas, it is essential to complete the final pass with a single tool to prevent surface mismatches. Another critical factor is the production volume: are you machining a highly specialized part that will be produced only once per engine, or a high-volume item like a door hinge of a passenger car?

Moreover, meeting timing requirements is crucial for a supplier aiming to be reliable. This involves assessing the manufacturing capacity relative to demand. Key considerations include the capacity of the production facility, the number of available machine centers, and whether parallel processing can be implemented to meet production targets efficiently.

MULTI OBJECTIVE With GENETIC ALGORITHM	BAYESIAN OPTIMIZATION With EXPLICIT WEIGHTS	NON-LINEAR CONSTRAINED OPTIMIZATION
Equally-weighted optimization for MRR and Tool Life A Trade-off point is calculated inside the algorithm	Roughing and Finishing Processes with different weight calculations ie. Roughing with max MRR ($W_{MRR}=100, W_{TL}=0$) Finishing with increased TL ($W_{MRR}=0, W_{TL}=100$)	When the tool is expensive When your surface is large to machine at one pass Briefly, when minimum tool life is a constraint
Multi Objective Optimization for complex non-linear problems Good at finding diverse set of solutions No explicit weight definition Pareto Front for the trade of the objective functions	Single Objective Function, ideal for expensive-to- evaluate problems Weight definition possible Scale differences require normalization Better for global optimum	A gradient-based optimization method best for constrained smooth non- linear problems Weight definition possible Efficiently finds local optimum
GAMULTIOBJ	BAYESOPT	FMINCON

Table 11: Comparison of the Optimization Methods

4.2.1 Genetic Algorithm for Multi Objective Optimization

Genetic algorithm is an optimization technique inspired of the process of natural selection. It is often applied to problems with multiple objectives, where the goal is to optimize two or more conflicting objectives simultaneously. In this study, it is selected due to its ability to define multi objective function to optimize. The objective function is complex or doesn't have a closed-form expression. The optimization landscape is non-linear and has multiple peaks or valleys.

You want to leverage a surrogate model (like GPR) for fast evaluation, which is especially beneficial for expensive simulations or experimental setups. However, it is not capable of explicitly defined weight inputs, it works with pareto chart which helps illustrate the trade-offs between multiple objectives in multi-objective optimization problems. The Pareto front consists of solutions where improving one objective would lead to a deterioration in at least one of the other objectives. In a 2D Pareto chart, one objective is plotted along the x-axis and another along the y-axis. Each point on the chart represents a solution, and the curve formed by the outer points represents the Pareto front.

$$\begin{aligned} f_1(x) &= \text{MRR}(x) \\ f_2(x) &= \text{ToolLife}(x) \end{aligned} \tag{4.3}$$

Maximize (MRR(x_i), TL(x_i))

4.2.2 Bayesian Optimization with Weight Definition

Bayesian optimization with a weighted sum approach is a robust method used to address multi-objective optimization problems, especially when objectives may conflict. In this

approach, each objective is assigned a weight reflecting its importance, and the weighted sum of all objectives forms a single objective function to optimize. By adjusting the weights, different trade-offs can be explored, providing flexibility to achieve desired outcomes based on priority.

To ensure comparability among objectives, normalization is often applied. Since each objective may operate on different scales, normalization methods help balance the influence of each objective within the weighted sum. Common techniques include *min-max normalization*, which scales each objective to a 0-1 range based on minimum and maximum values, and *z-score normalization*, which standardizes objectives based on mean and standard deviation, ensuring they have a comparable influence in the optimization process. *Objective scaling* directly adjusts objective values relative to their magnitude, while *adaptive scaling* dynamically re-weights objectives throughout the optimization process to improve convergence toward a balanced solution. Another approach, *penalty-based normalization*, penalizes objective values that deviate substantially from targets, aiding in finding feasible solutions in constrained environments.

Selecting an appropriate normalization method can significantly impact the optimization's performance, helping ensure that the Bayesian optimization process converges toward solutions that reflect the intended priorities among objectives.

$$\begin{aligned} \max_x (w_1 f_1(x) + w_2 f_2(x)) \\ f_1(x) = \text{MRR}(x) \\ f_2(x) = \text{ToolLife}(x) \end{aligned} \tag{4.4}$$

4.2.3 Non-linear Constrained Optimization

This optimization is used in a specific condition where tool life is limited with a minimum value while maximizing MRR to complete finish pass with at least one tool. Hence, one more constraint is added to the finishing constraint. The objective function function is the same with Bayesian approach with this one additional limitation as shown in Eqn. 4.7.

4.3 Constraint Definition

Constraint definition is another important step to establish a feasible solution set and save computational time. The upper and lower limits of the cutting parameters were determined according to the machine tool limits, the tool manufacturer's data and design requirements.

The constraints for roughing process

$$\begin{aligned} \text{Power} &\leq 86000 \text{ watts} \\ \text{Torque} &\leq 26000 \text{ Nm} \\ \text{Tool Bending Stress} &\leq 1533 \text{ MPa} \\ X_i > 0 \quad \text{and} \quad Y_i > 0 \quad \text{for} \quad i = 1, 2, 3, \dots \end{aligned} \tag{4.5}$$

The constraints for finishing process

$$0.8 * \text{Design Tolerance} \leq Y_6(x_i) \leq \text{Design Tolerance} \quad (4.6)$$

$$\text{Required machining time for finish pass} \leq Y_2(x_i) \quad (4.7)$$

$$X_i > 0 \quad \text{and} \quad Y_i > 0 \quad \text{for} \quad i = 1, 2, 3, \dots$$

The constraints for testing process

$$0 \leq x_1 \leq 8 \text{ mm (axial depth of tool catalog)}$$

$$0.003 \leq x_3 \leq 0.085 \text{ mm/rev*tooth (max feed rate of tool catalog)} \quad (4.8)$$

$$x_5 = 2 \text{ (fixed flute number)}$$

4.3.1 Feed per Tooth Limits

The minimum uncut chip thickness was limited based on the tool hone radius, which is suggested to be at least 0.3 times the hone radius (i.e., $h_{min}=0.3*R_{hone}$) [28]. Figure 2 illustrates hone radius measurement via Nano-focus μ -surf device.

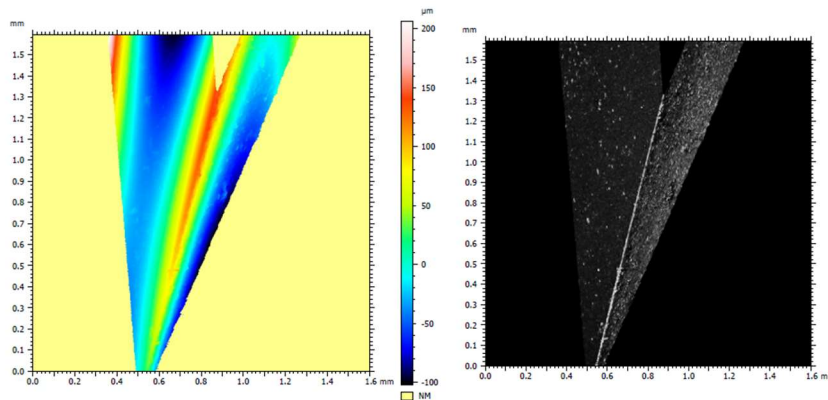


Figure 12: Hone radius measurement using Nano-focus μ -surf explorer.

The maximum uncut thickness is selected on the tool catalogue, for 16-mm diameter as shown in Figure 13.



	1/1	1/2	1/5
Kesme değerleri			
Kesme hızı (v_c)	32.8 m/min	34.2 m/min	35.1 m/min
Diş başı ilerleme (f_z)	0.0684 mm	0.0684 mm	0.0855 mm
Ayar açısı	90°		
Maksimum kesme derinliği (a_p)	8 mm		
Kesici uç tipi	AD.080304		

Figure 13: Tool Catalog for Feed Rate Upper Limit

4.3.2 Power and Torque Limits of Machine Center

Power and torque are calculated by equation (2.16) and their limits are derived from the machine tool's power and torque curves, as illustrated in Figure 3 for Mazak Nexus 510 CII Milling Center (12.000rpm).

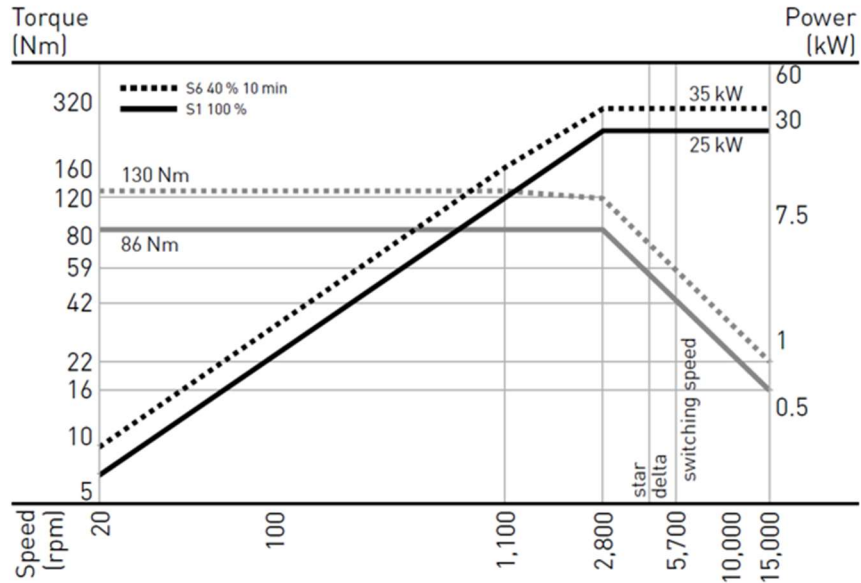


Figure 14. Power/torque curve of Mazak Nexus 510 CII Milling Center.

4.3.3 Axial Depth of Cut Limits

Axial depth of cut is dependent on tool cutting length as shown in Figure 13. The upper bound of axial depth is set to 8mm.

4.3.4 Radial Depth of Cut Limits

Radial depth of cut is taken as percentage, it is defined as 10% and 100% of radial immersion. For the diameter of 16mm, its lower bound results in 1.6mm and upper bound is the diameter itself as full immersion.

4.3.5 Spindle Speed Limits

The cutting speed for Titanium alloy practically varies 400m/min, meaning that with a 16mm diameter tool, spindle speed is approximately 6700 rpm. For a larger scan of optimum solution, the upper bound is set to 5000 rpm and lower bound is 1000rpm since the experiment will be under dry cutting conditions.

4.3.6 FRF Measurement

Prediction of chatter occurrences is one of the important steps for the optimization process because it adversely may cause the waste of workpiece and may damage the machine center. Due to the periodic nature of milling operations, cutting force varies with the angle of the cutting edge. Furthermore, the number of actively cutting teeth, whether one or more edge is cutting at in instance regarding the radial depth percentage and flute number affects the cutting forces with the rotation of the spindle. These forces are acting like external excitation that can be considered as forced vibration, and they are a combination of sinusoidal forces. Fourier transform is utilized to the amplitude and the frequency content of these forces. The variation of the cutting forces additionally results in the variation of chip thickness and the vibration of the tool may be diminished or grown with successive tooth entry to the workpiece.

A brief historical development of chatter stability modeling begins with Tlustý's average cutting direction approach [36], and he continued his studies that indicate that time domain simulations are more effective for stability modeling. Budak [37] has established an analytical stability method, verified experimentally and numerically. Later, this method was extended for stability lobe diagram generation and even for 3D stability analysis. [37,38,39,40].

Since this thesis is focused on milling operation optimization with one specific carbide cutting tool with 16-mm diameter as 2-fluted square end mill, the effect of tool length [41]

or the special tool parameters such as variable pitch or serrated geometries have not been considered [42,43]. In this thesis, stability diagrams have been generated with the input of hammer test processed with Fast-response-function (FRF) by using receptance coupling and substructure analysis (RCSA) [44,45].

FRF measurement is the main part of the chatter mitigation since it enables the machinist to generate stability diagram and identify the chatter-free limits for spindle and radial depth pair. Tool length is measured as 75 mm and hammer impacts are applied to the tool tip.



Figure 15: PCB Piezotronics Modal Analysis Sets

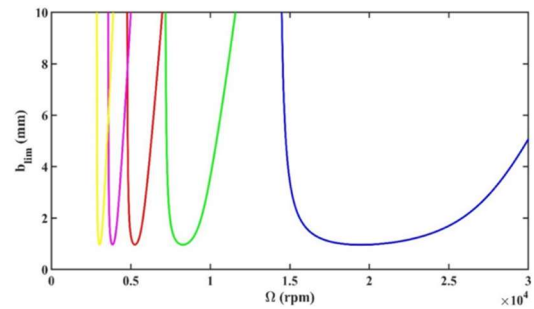
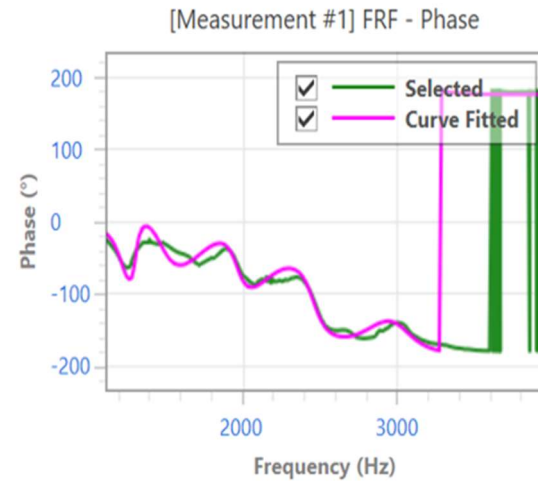
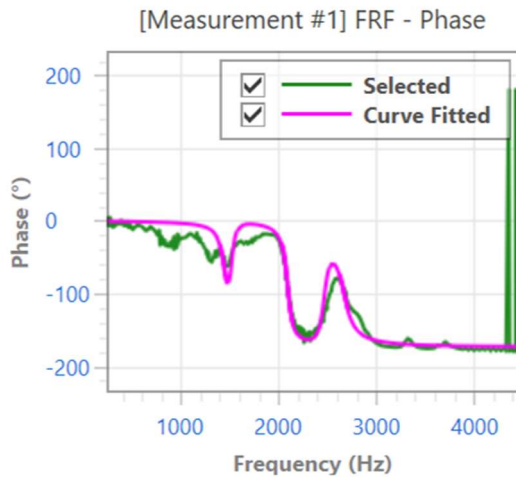
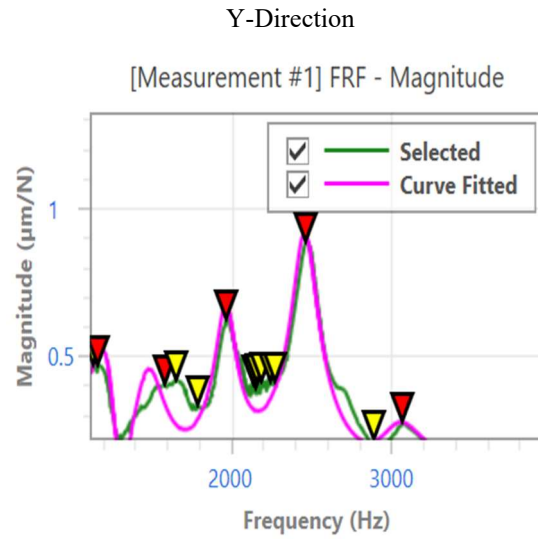
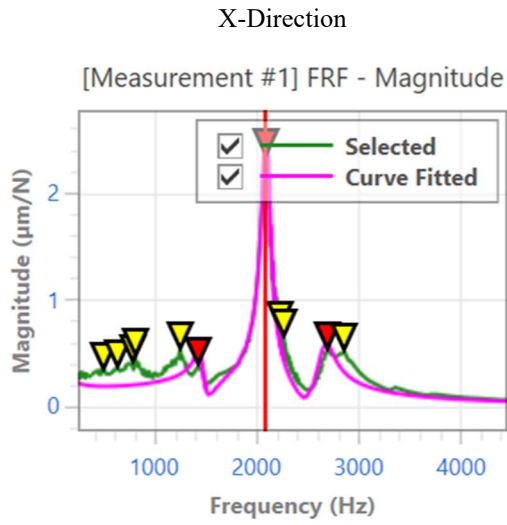


Figure 16. Stability lobe diagram



Optimized Modes

Optimized Modes

Mode No:	Frequency [Hz]	Damping Ratio [%]	Modal Stiffness [N/m]	Modal Mass [kg]
1	1445.05	3.47	3.5125E07	0.426
2	2088.09	1.92	1.0262E07	0.060
3	2663.81	3.20	2.8003E07	0.100

Mode No:	Frequency [Hz]	Damping Ratio [%]	Modal Stiffness [N/m]	Modal Mass [kg]
1	1231.45	5.72	1.8637E07	0.311
2	1480.16	7.13	3.1118E07	0.360
3	1966.39	3.49	3.2035E07	0.210
4	2459.31	3.33	1.9843E07	0.083
5	3042.40	5.06	7.5432E07	0.206

Table 12: FRF Measurement Results to select chatter free solutions

4.3.7 Design Tolerance Limits

Tolerance input is directly related to the design intent of the milling surface. According to the function of the milling surface, tolerance bands are indicated in the technical drawings. For this optimization approach, tolerance band is not in the constraint list but will be used during the iterations for best solutions.

Furthermore, it is quite critical that finishing operation must be completed without tool change since this can cause any mismatch line on the surface and successively the rejection of the part.

In this optimization problem, absolute value of the form error has been considered if the milling surface has a bilateral profile tolerance. When the design has unilaterally defined profile tolerances, the direction of the form error will be important since it will indicate stock-off or stock-on condition.

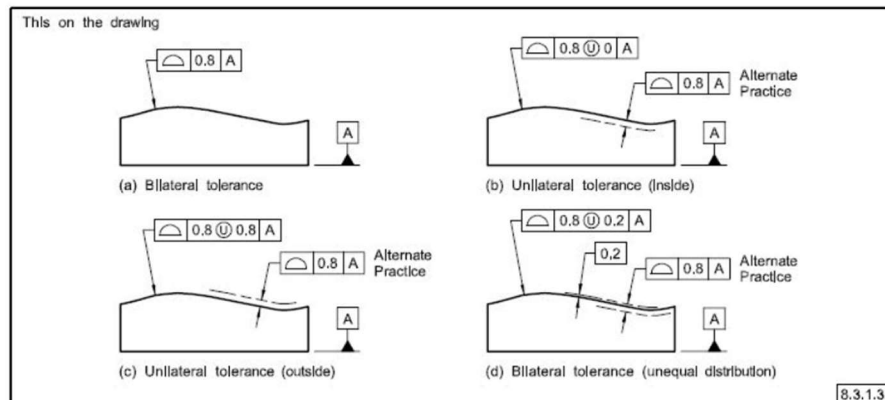


Figure 17. application of surface profile tolerance on a basic contour

5. Results

The optimization of machining parameters was conducted using 3 different algorithms and Gaussian process regression, with the aim of maximizing productivity and mitigating chatter, as outlined in Equation (5). According to the upper and lower band limits of the input parameters (axial/radial depth of cut, feed rate, spindle speed and teeth number), the optimization process aimed to maximize material removal rate and tool life, while ensuring power/torque limits and tool breakage constraints for roughing as well addressing form error for finishing. This comprehensive approach ensures that the process is both efficient and cost-effective, leading to improved productivity and profitability without compromising the life span of the cutting tools used.

Initially, the cutting forces used for the calculation of power consumption, torque and bending stress were estimated using a physics-based ML model, which predicts the milling forces with high level of accuracy [24]. After dataset preparation, the hyperparameter optimization of Gaussian Process Regression (GPR) was performed, as summarized in Table 2.

5.1 Multi-Objective Optimization with Genetic Algorithm

Regarding many machining scenarios as described in Chapter 4.2, this multi-objective optimization allows the manufacturer to follow an equally weighted solutions when no timing or volume restrictions exist.

This code aims to find optimal values for the inputs x_1 , x_2 , x_3 , and x_4 that maximize MRR (Y_1) and Tool Life (Y_2). Since *gamultiobj* is a minimization function, we use the negative values of Y_1 and Y_2 (minimizing $-Y_1$ and $-Y_2$) to achieve maximization.

The constraints are based on predicted values of power (Y3), torque (Y4), tool bending stress (Y5) and form error (Y6). Depending on the process type (roughing or finishing), the constraints on these outputs differ. For example:

- In roughing, constraints are:
 - Power < 86000 Watts
 - Torque < 26000 Nm
 - Tool Bending Stress < 1533 MPa.

- In finishing:
 - 0.04 mm < Form Error < 0.05 mm.

The code optimizes four variables: axial and radial depth, feed per tooth, and spindle speed. The variable of flute number is fixed at 2 at this point since the tool is consolidated, allowing the model to focus on the primary four variables. The upper and lower boundaries for these variables are specified as

- x_1 : [0, 8] → Tool axial depth limitation
- x_2 : [0, 16] → Limited by tool radius
- x_3 : [0.003, 0.085] → → limited by tool hone radius and tool catalog
- x_4 : [0, 5000] → reasonable interval for titanium-carbide pair.

These bounds ensure the search space is constrained to feasible ranges, which can significantly influence the optimizer's performance.

The objective function, `gprObjective`, takes the four optimization variables (x_1 to x_4) and appends a fixed x_5 value of 2, making it a complete 5-element vector for prediction. The function uses the Gaussian Process Regression (GPR) model and another machine learning model (e.g., `lsboostModel`) to predict Y_1 and Y_2 based on x_i .

The function returns `[-Y1_pred, -Y2_pred]`, thereby converting the maximization of Y_1 and Y_2 into a minimization problem, which aligns with `gamultiobj` requirements. The `gamultiobj` function is a genetic algorithm tailored for multi-objective problems. It uses

population-based search, which simulates evolution through operations like mutation, crossover, and selection. The `opts` structure specifies options such as `Display`, set to 'iter' to show progress at each iteration, and `PlotFcns`, which includes `@gplotpareto`. This function plots the Pareto front (showing trade-offs between objectives) during optimization.

By default, `gamultiobj` will iterate over several generations to evolve a set of solutions. The exact number of generations can depend on factors like population size, convergence criteria, and stopping conditions (such as maximum generation count). Each generation produces a population of potential solutions that are tested and refined.

`gamultiobj` generates a set of solutions that represent trade-offs between the objectives Y_1 and Y_2 . This set, the Pareto front, comprises solutions where no single solution is strictly better in all objectives than any other (known as “non-dominated” solutions). During the optimization, the convergence plot shows how solutions improve over generations, helping to visualize how quickly or smoothly the algorithm reaches good solutions. After optimization, `gamultiobj` returns a set of solutions (`x_opt`) and corresponding objective values (`fval`). These represent various trade-offs between Y_1 and Y_2 on the Pareto front.

The solutions are sorted based on the objective values, allowing the code to select the “best” 20 solutions which will be the input for detecting the chatter condition and filtering respectively. The Pareto front may help the manufacturer to select among possible parameters regarding the balance between Y_1 and Y_2 and their priorities such as prioritizing Y_1 over Y_2 or vice versa.

The results of genetic algorithm is not so promising when compared to Bayesian optimization. For roughing, it suggested a balanced solution set where it increased depths while decreasing feed rate and spindle speed or vice versa.

Axial depth of cut (mm)	Radial depth of cut (mm)	Feed per tooth	Spindle speed (rpm)	Tooth number	MRR (mm³/min)	Tool life (min)	Power (w)	Torque (N.mm)	Bending stress (MPa)
0.1	5.9	0.026	3000	2	92	4.6	37.7	53	0.45
1.4	7.3	0.003	1000	2	61	1.2e6	41.5	326	5.5
0.2	3.8	0.023	1000	2	35	665	21	92	0.8
0.1	3.9	0.065	1000	2	50.7	14.8	37	95	0.6

Table 13: Roughing Solutions from Genetic Algorithm

For finishing operation, the code recommended much higher axial and radial depth than the common practice in industry.

Axial depth of cut (mm)	Radial depth of cut (mm)	Feed per tooth	Spindle speed (rpm)	Tooth number	MRR (mm³/min)	Tool life (min)	Power (w)	Torque (N.mm)	Bending stress (MPa)
3.38	6.25	0.038	1001	2	1607	105	651	2352	20.9
5.45	9.5	0.026	3000	2	8077	4.6	2080	2996	36.8

Table 14: Finishing Solutions of Genetic Algorithm

5.2 Bayesian Optimization with Explicit Weight Definition

Regarding the different machining requirements described in Chapter 4.2 and the limitations of genetic algorithm, Bayesian optimization method has been investigated since it allows explicit weight definition for each optimizer. Both roughing and finishing

operations may demand more productivity or longer tool life in different conditions. Since weight definitions lead in the weighted sum approach, the scale of each optimizer is inevitable requires a normalization step. 5 different normalization techniques have been used and compared to understand which approach is more reliable and repeatable.

The weighted sum approach targets to optimize Material Removal Rate (MRR) and Tool Life (TL)—represented by Y1 and Y2, meaning that the objective function combines Y1 and Y2 using predefined weights w_1 and w_2 , respectively. The summation of these weights is set to 100 (or 1.0, when normalized) to maintain consistency. Bayesian approach, as many other optimization algorithms, minimize rather than maximize, hence the scaled objective function is represented as *minimize* $-(w_1 \cdot \text{scaled } Y1 + w_2 \cdot \text{scaled } Y2)$.

The raw predictions for Y1 and Y2 (obtained through Gaussian Process Regression and LS-Boost models) may differ significantly in scale. To ensure a fair comparison and combination, each objective has been scaled before applying the weights. This way, both objectives contribute meaningfully regardless of their magnitude, aligning their values closer and mitigating the impact of one variable's natural scale over the other. The choice of weights w_1 and w_2 determines the relative importance of each objective. A higher weight on Y1 (MRR) means the optimization process will prioritize maximizing material removal rate, while a higher weight on Y2 (TL) will favor maximizing tool life. By adjusting w_1 and w_2 , you can explore trade-offs, such as achieving a high MRR with acceptable tool life or prioritizing longevity at the expense of material removal.

The constraints are the same as genetic algorithm and based on predicted values of power (Y3), torque (Y4), tool bending stress (Y5) and form error (Y6). Depending on the process type (roughing or finishing), the constraints on these outputs differ. For example:

- In roughing, constraints are:
 - Power < 86000 Watts
 - Torque < 26000 Nm
 - Tool Bending Stress < 1533 MPa.

- In finishing:
 - 0.04 mm < Form Error < 0.05 mm.

The code optimizes four variables: axial and radial depth, feed per tooth, and spindle speed. The variable of flute number is fixed at 2 at this point since the tool is consolidated, allowing the model to focus on the primary four variables. The upper and lower boundaries for these variables are specified same as genetic algorithm as

- o x1: [0, 8] → Tool axial depth limitation
- o x2: [0, 16] → Limited by tool radius
- o x3: [0.003, 0.085] → → limited by tool hone radius and tool catalog
- o x4: [0, 5000] → reasonable interval for titanium-carbide pair.

Since normalization is quite critical for reasonable solutions, 5 common normalization techniques have been tried and compared.

- Min-Max Normalization scales each objective to a specific range [0,1], the critical limitation of this approach is that it is very sensitive to outliers.

$$Y_{\text{scaled}} = \frac{Y - Y_{\min}}{Y_{\max} - Y_{\min}} \quad (5.1)$$

- Z-score Normalization scales data based on its mean and standard deviation, resulting in a distribution with a mean of 0 and standard deviation of 1.

$$Y_{\text{scaled}} = \frac{Y - \mu}{\sigma} \quad (5.2)$$

- Objective-Specific Scaling adjusts each objective by factors relevant to its practical interpretation, such as typical ranges, limits, or target values specific to each objective. Fine-tuning that aligns normalization with domain-specific insights, ensuring that the scaled objectives contribute meaningfully to optimization is the strength of this algorithm.

- Adaptive Scaling (Dynamic Range Adjustment) is like min-max but recalculated iteratively as the optimization progresses.

$$Y_{\text{scaled}} = \frac{Y - Y_{\text{min, current}}}{Y_{\text{max, current}} - Y_{\text{min, current}}} \quad (5.3)$$

- Penalty-Score Scaling introduces penalties for deviations from desired values or ranges, often rewarding values within a specified range. It is useful when specific constraints or ranges are critical to optimization.

$$Y_{\text{scaled}} = \begin{cases} 1 - \left| \frac{Y - Y_{\text{target}}}{Y_{\text{acceptable range}}} \right|, & \text{if } Y \text{ is within range} \\ \text{penalty}, & \text{if } Y \text{ is out of range} \end{cases} \quad (5.3)$$

Matlab code block for Bayesian optimization for multi-objective optimization results:

```
bayesopt(objectiveFcn, vars, 'IsObjectiveDeterministic', true, ... 'NumCoupledConstraints', 0, 'PlotFcn', @plot, ... 'AcquisitionFunctionName', 'expected-improvement-plus', ... 'UseParallel', true, 'MaxObjectiveEvaluations', 20, ... 'Verbose', 1);
```

objectiveFcn: The function that evaluates the objectives you want to optimize is described with this function. Either a single-objective or multi-objective function can be solved depending on your use case. The function generates an acceptable set of variables and returns the objective value(s).

vars: The variables being optimized is defined here, typically using `optimizableVariable`. For example, `vars = [optimizableVariable('x', [0, 1]), optimizableVariable('y', [0, 5])]`.

IsObjectiveDeterministic: This parameter is set to true here, indicating that the objective function is deterministic (i.e., it always returns the same value for the same input). If your objective function is random, it needs to be set as false.

NumCoupledConstraints: This parameter is set to 0 here, meaning there are no coupled constraints on the optimization, meaning that the constraints are defined independently of each other, not in a relationship.

PlotFcn: This input is indicating the demand for the plotting function for displaying progress. Here, @plot is used. MATLAB's bayesopt offers other plot options, such as @plotMinObjective for the minimum objective value.

AcquisitionFunctionName: This sets the acquisition function used to explore the objective function's unknown landscape. Expected-improvement-plus is a popular acquisition function that balances exploration and exploitation.

UseParallel: In this study, it is set to true, meaning Bayesian optimization will evaluate points in parallel if possible. This is useful if you have multiple cores available or if running on a cluster.

MaxObjectiveEvaluations: The maximum number of objective function evaluations (in this study, 20 solutions). Any increase in this parameter may yield better optimization results but will take more computational time.

Verbose: It is set to 1 to Control the level of output to the command line, which provides basic information on the optimization's progress. Using higher values will provide more detailed output.

Sensitivity analysis

Sensitivity analysis is performed to understand how the changes of input parameters affect the outputs. This algorithm estimates which parameters is dominant on each output so that decision making process will be clearer. For example, the optimization of tool life is not affected by the depths of machining process, it is dependent on feed rate and spindle speed. Hence, any adjustment on tool life can be achieved with the change only in these two parameters, not with the depth of cut or flute number. Sensitivity analyses help the operator select among optimized solutions for any specific case of milling process.

Axial depth of cut (mm)	Radial depth of cut (mm)	Feed per tooth	Spindle speed (rpm)	Operation (R / F)	Weight for MRR	Weight for Tool Life	Scaling Type
3.5	13.5	0.07	4713	R	100	0	Adaptive
7.2	15.6	0.04	2074	R	100	0	Adaptive
7.7	13.7	0.049	2021	R	100	0	Min-max
7.6	14.1	0.018	4153	R	100	0	Min-max
6.5	11.5	0.065	4638	R	100	0	Objective
7.2	13.2	0.041	4355	R	100	0	Objective
4.15	12.03	0.083	2794	R	100	0	Penalty
7.08	4.58	0.071	4823	R	100	0	Penalty
7.0	11.2	0.079	2574	R	100	0	z-Score
3.7	11.9	0.073	4341	R	100	0	z-Score
6.3	9.2	0.015	527	R	0	100	Adaptive
3.6	12.4	0.044	375	R	0	100	Adaptive
7.6	7.8	0.021	472	R	0	100	Min-Max
4.7	9.2	0.011	931	R	0	100	Min-Max
3.8	13.9	0.010	296	R	0	100	Objective
4.8	3.8	0.005	781	R	0	100	Objective
7.0	12.6	0.010	539	R	0	100	Penalty
2.0	15.2	0.006	1296	R	0	100	Penalty
0.6	11.6	0.006	379	R	0	100	z-Score
6.7	0.3	0.001	4740	R	0	100	z-Score

Table 15. Best two optimal solutions per each normalization technique for a chatter-free roughing operation with different weight definitions

Best Solutions Scatter Plot For Roughing Operation with $W_{MRR}=0$, $W_{TL}=100$

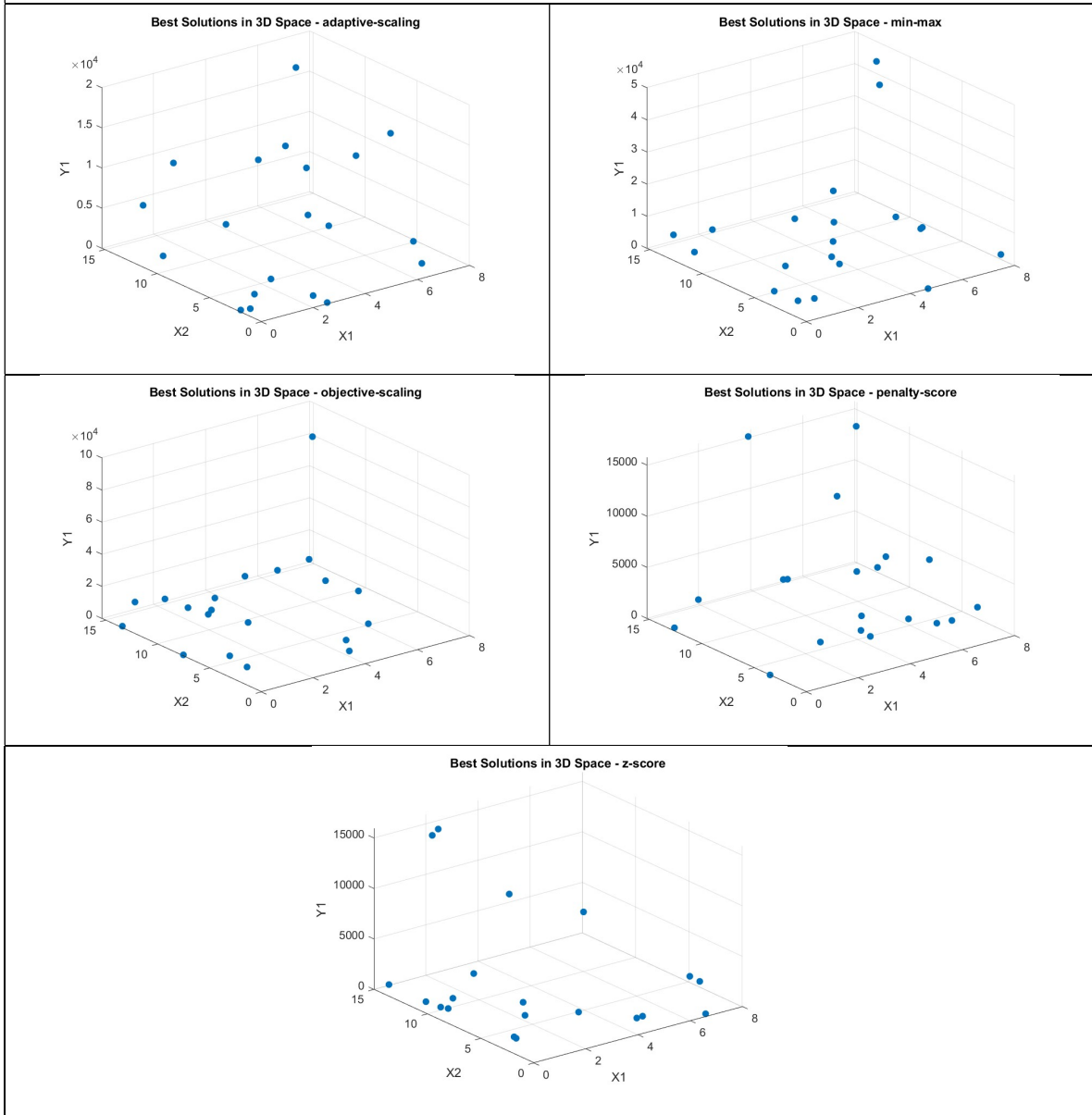


Table 16: Best Solutions Scatter Plot for Roughing Operation with $W_{MRR}=0$, $W_{TL}=100$

Best Solutions Scatter Plot For Roughing Operation with $W_{MRR}=100$, $W_{TL}=0$

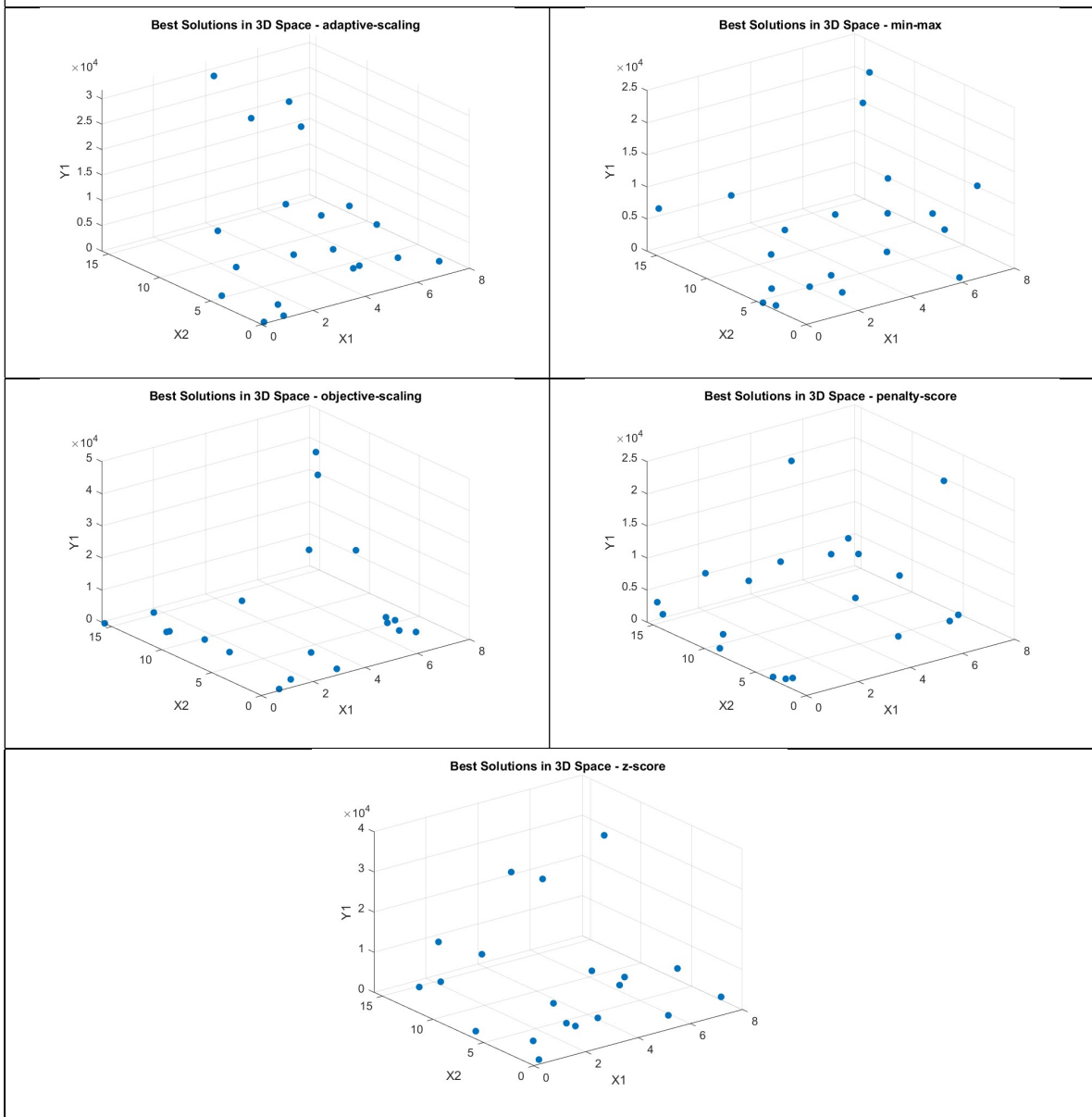


Table 17: Best Solutions Scatter Plot for Roughing Operation with $W_{MRR}=100$, $W_{TL}=0$

Axial depth of cut (mm)	Radial depth of cut (mm)	Feed per tooth	Spindle speed (rpm)	Operatio n (R / F)	Weight for MRR	Weight for Tool Life	Scaling Type
3.5	3.0	0.044	3521	F	100	0	Adaptive
5.8	5.5	0.067	422	F	100	0	Adaptive
6.8	4.3	0.053	3604	F	100	0	Min-max
4.3	10.3	0.028	1595	F	100	0	Min-max
4.4	1.2	0.081	638	F	100	0	Objective
1.8	1.7	0.020	2651	F	100	0	Objective
2.4	1.6	0.077	2538	F	100	0	Penalty
0.4	6.4	0.085	1179	F	100	0	Penalty
1.1	6.6	0.077	2849	F	100	0	z-Score
0.7	6.5	0.033	2320	F	100	0	z-Score
7.3	0.2	0.014	913	F	0	100	Adaptive
5.3	1.3	0.010	1324	F	0	100	Adaptive
0.4	5.9	0.081	352	F	0	100	Min-Max
0.9	16.0	0.031	924	F	0	100	Min-Max
1.6	2.8	0.002	3504	F	0	100	Objective
0.4	1.2	0.007	2130	F	0	100	Objective
0.2	12.3	0.024	1302	F	0	100	Penalty
1.9	1.3	0.043	893	F	0	100	Penalty
0.01	11.5	0.002	615	F	0	100	z-Score
4.5	12.0	0.003	522	F	0	100	z-Score

Table 18: Best two optimal solutions per each normalization technique for a chatter-free finishing operation with different weight definitions

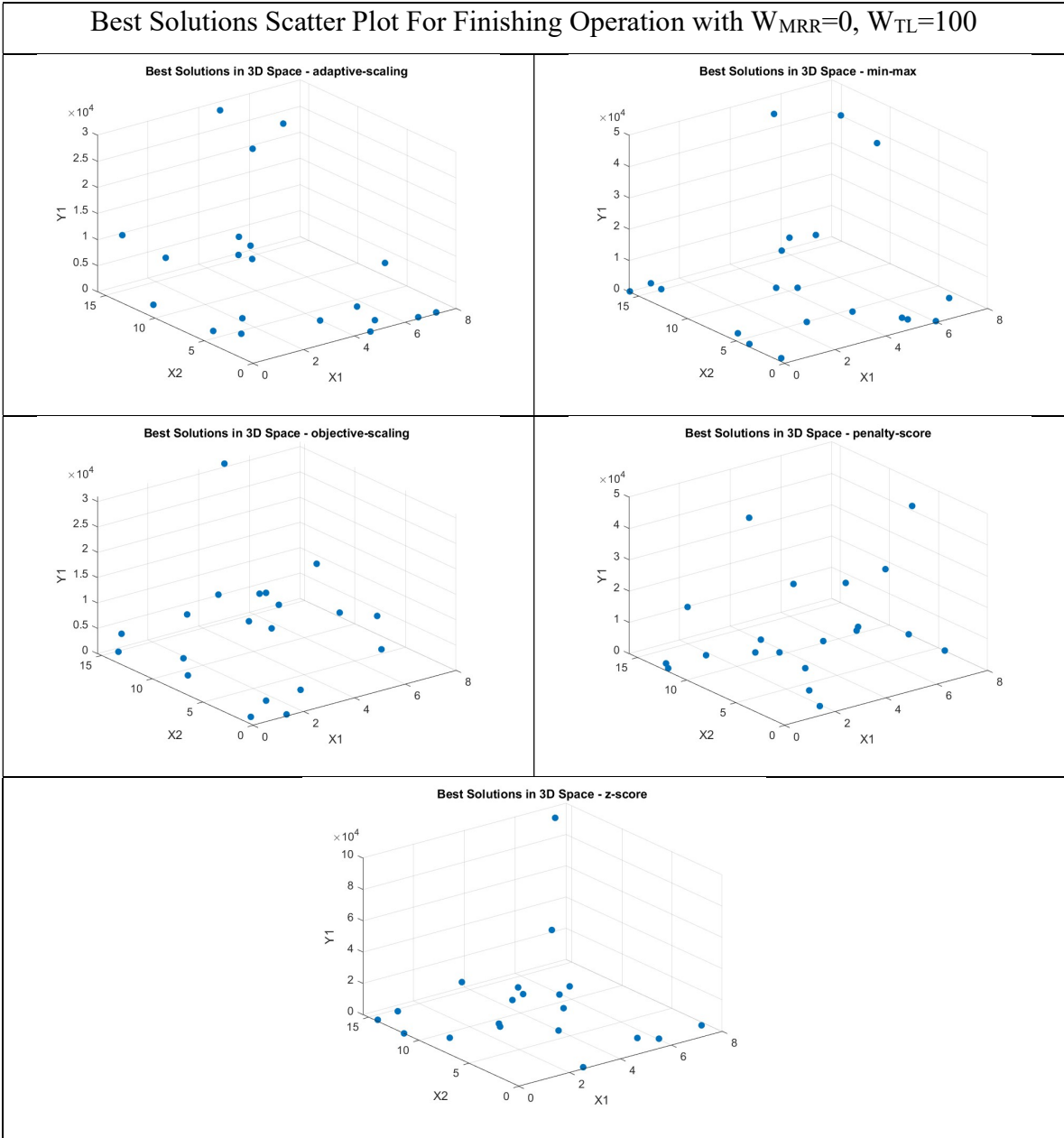


Table 19: Best Solutions Scatter Plot for Finishing Operation with $W_{MRR}=0$, $W_{TL}=100$

Best Solutions Scatter Plot For Finishing Operation with $W_{MRR}=100, W_{TL}=0$

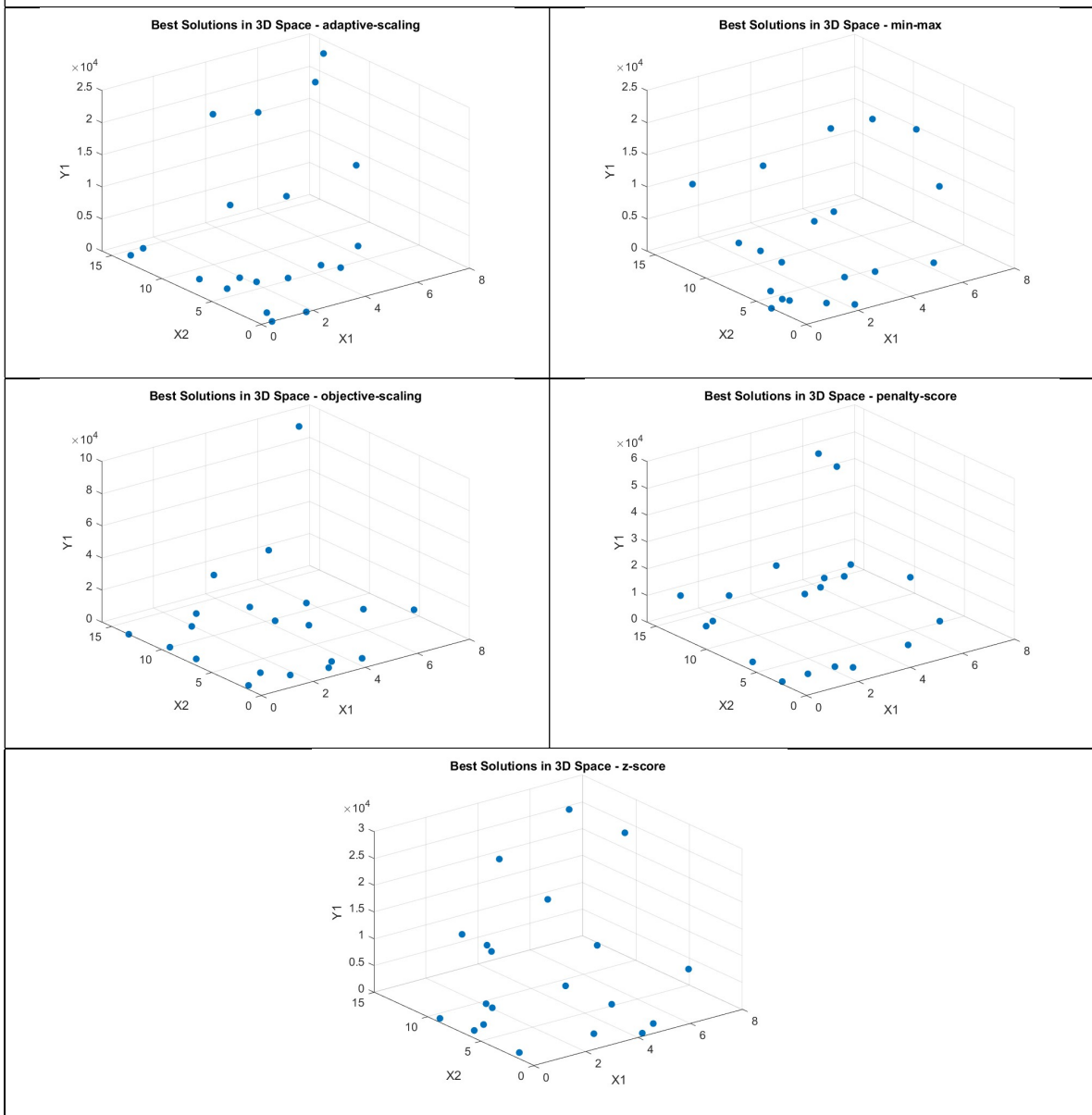


Table 20: Best Solutions Scatter Plot for Finishing Operation with $W_{MRR}=100, W_{TL}=0$

5.3 When Tool Life has a minimum machining time

When the machinist has to achieve a certain machining time for finishing operation of a large surface not to leave any mismatch line on the surface, the optimization problem turns into a new type problem that requires a specific solution: a parameter is defined in both objective function and constraints. Both Bayesian and nonlinear constrained optimization are applicable to this specific requirement. One more additional constraint for finishing has been added to the formulation:

$$\text{minimize } -(w1 \cdot Y1_{scaled} + w2 \cdot Y2_{scaled})$$

- *Subject to*
 - $0.04 \text{ mm} < \text{Form Error} < 0.05 \text{ mm.}$
 - $0 \text{ min} < Y2 < 300 \text{ min}$

As seen in the Table 20 and 21 showing the best solution results and scatter plots, Bayesian optimization can still offer diverse solution set, however nonlinear constrained optimization approach ends up with only one optimal solution. The weakness of this nonlinear constrained approach is that it can be stuck in local optimum and results are very dependent on the initialization point. Hence, it should be iterated more than once before decision making about parameters.

Axial depth of cut (mm)	Radial depth of cut (mm)	Feed per tooth	Spindle speed (rpm)	Optimizer	Scaling Type
1.9	0.7	0.067	1831	Bayesian	Adaptive
0.6	11.1	0.012	1313	Bayesian	Min-max
0.6	7.3	0.045	1233	Bayesian	Objective
1.3	1.9	0.026	687	Bayesian	Penalty
1.8	12.3	0.032	540	Bayesian	z-Score
4	8	0.04	2500	Nonlinear Constrained	All Types

Table 21: Best Solutions for Finishing Operation with min machining time constraint and $W_{MRR}=0$, $W_{TL}=100$ with different scaling techniques

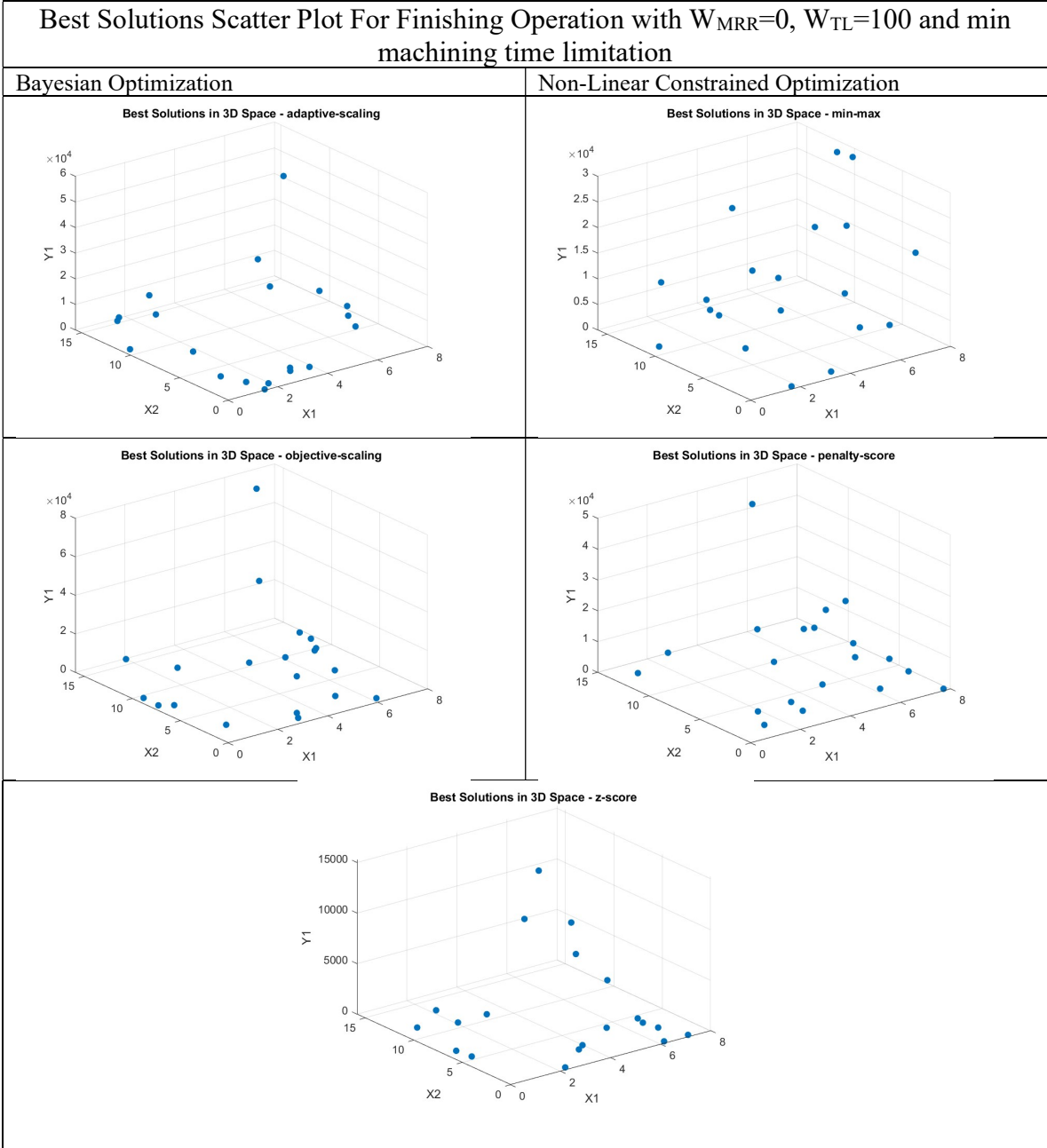


Table 22: Best Solutions Scatter Plot for Finishing Operation with $W_{MRR}=0$, $W_{TL}=100$ and min machining time limitation solved with Bayesian Optimization

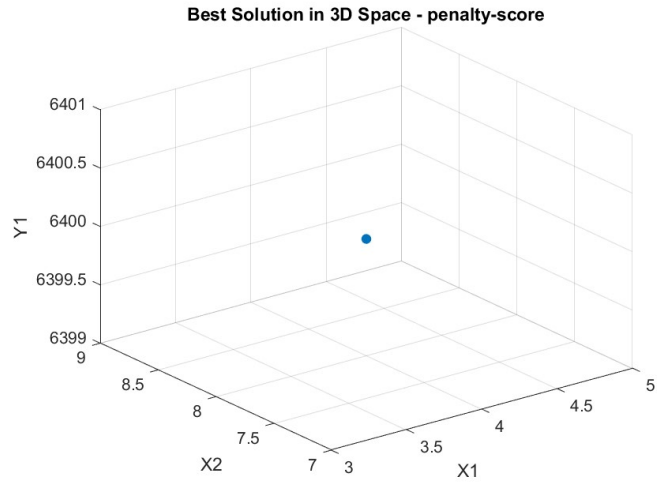


Figure 18: The best Solutions Scatter Plot for Finishing Operation with WMRR=0, WTL=100 and min machining time limitation solved with Nonlinear Constrained Optimization

6. Experimental Verification

6.1 Cutting Tool

For testing, a cutting tool with 16mm diameter, 2 flute inserted carbide tool has been selected, which is capable of cutting Ti6Al4V material (HB~330-375) described with S7 code. The codes for the tool and the insert has been listed in Table 22.

Cutting Tool	Walter F4042.Z16.016.Z02.08
Cutting insert	Walter ADMT080308R-F56 WSP45S

Table 23: The codes for the cutting tool



Figure 19: The cutting tool on machining center

6.2 Parameter Selection for Testing

The results used for testing purpose was selected by Bayesian Optimization process. Regarding the trend that tool life extension directs the operator to select lower spindle speed and feed rate with one higher and one lower depth, rounded values of different scalings has been used as shown in the Table 24. One higher and one lower depth can be used interchangeably since the optimum value will not be effected. The operation type such as profiling or pocketing may help the operator decide efficiently.

In contrast, higher MRR requirement generally tends to select higher depths and spindle speed with lower feed rate. Here in this scenario, productivity rate has been increased by 14 times, however tool lif has been decreased by 80%. This is valid when tool is really cheap and scrapable.

Assuming that spindle speed can be lowered by half, the operation will still have 7 times improvement and tool life can be still preserved respectively.

	a	b	f	N	MRR	Tool Life	Form Error	Wear
Roughing								
Tool Life-Optimized	8	0.1	0.085	700	95.2	43	0.011	163
MRR Optimized	2.5	8	0.02	1750	1400	7.4	0.110	144
Finishing								
Tool-Life Optimized	0.3	0.5	0.05	1200	18.2	58	x	x
MRR Optimized	0.5	1.7	0.03	1450	63	63	x	x

Table 24: Summary for Test Results for both MRR and Tool-Life Optimizes solutions

6.3 Measurements

The machine center used for the cutting test is shown in Figure-21.



Figure 20: Mazak Nexus 510 CII Milling Center (12.000rpm)

6.3.1 Force Measurement

For the force measurement, the equipment to measure the forces is shown in Figure-22.



Figure 21: Kistler Piezo-Dynamometer with Large Measuring Range

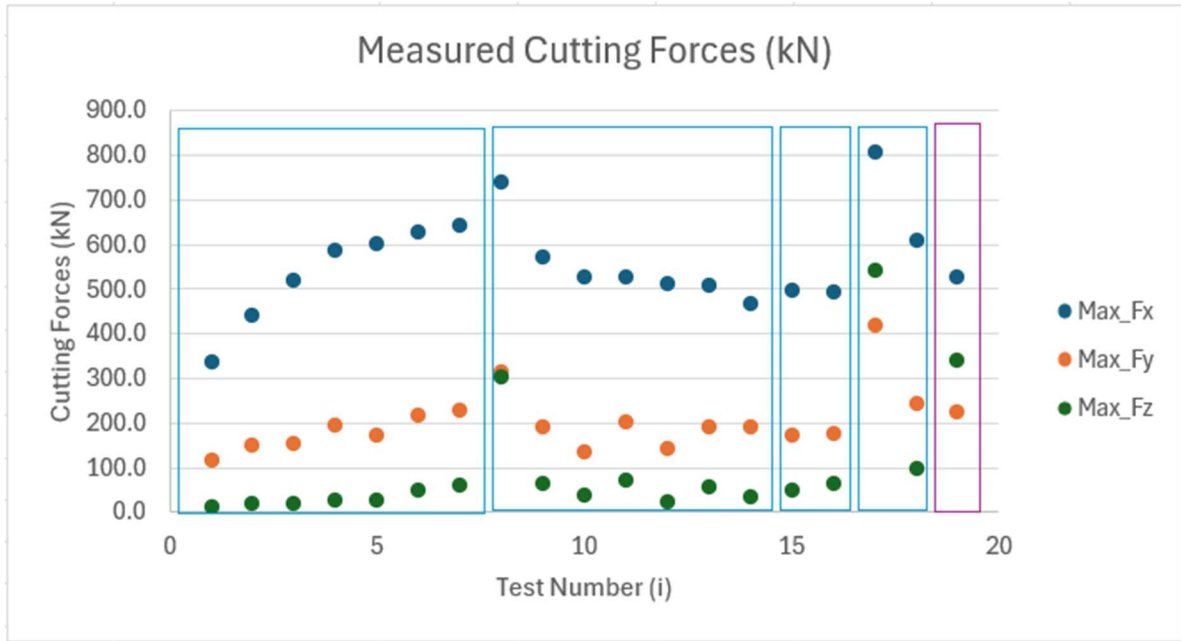


Figure 22: Cutting Force Plot

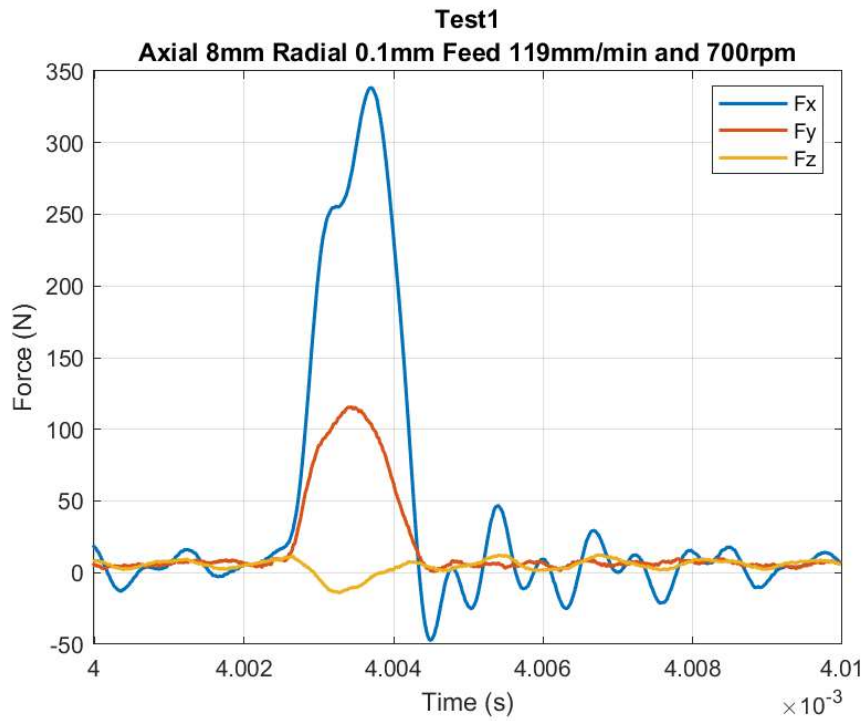


Figure 23: The Cutting Forces for Tool-Life Optimized Experiment

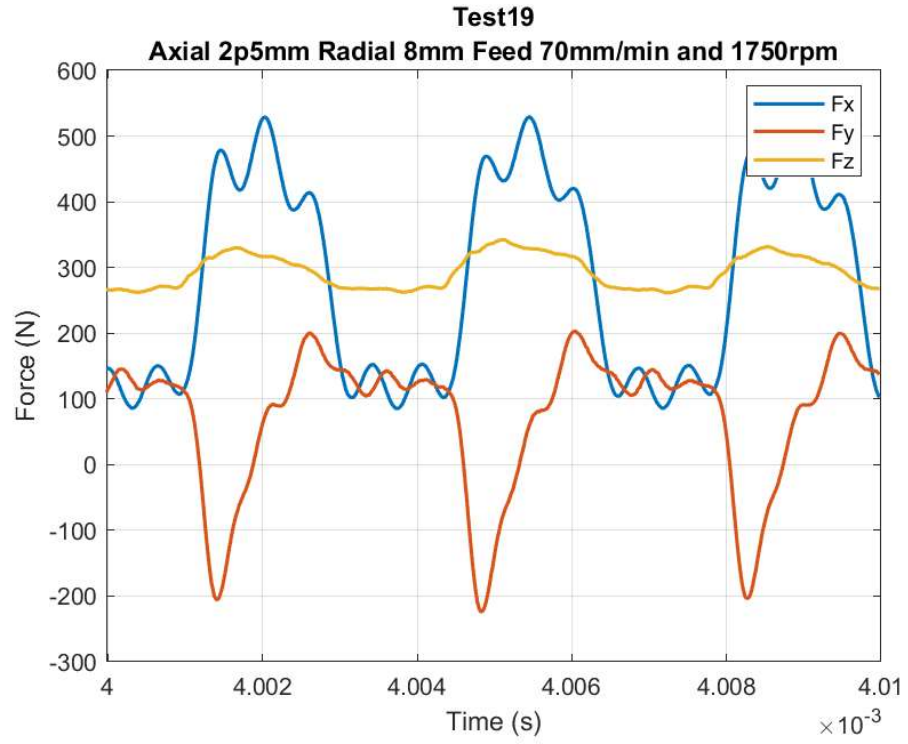


Figure 24: The Cutting Force Measurement for MRR-Optimized Test

The forces of the tests are listed below in the Table-25.

	mm	mm	mm/tooth	mm/min	rpm			
Test No	Axial	Radial	Feed	Feed	S.Speed	Max_Fx	Max_Fy	Max_Fz
0						4.5	6.5	6.0
1	8	0.1	0.085	119	700	338.4	115.8	14.0
2	8	0.1	0.085	119	700	443.7	149.3	19.2
3	8	0.1	0.085	119	700	520.3	155.4	21.1
4	8	0.1	0.085	119	700	588.6	195.3	25.6
5	8	0.1	0.085	119	700	602.8	174.1	26.6
6	8	0.1	0.085	119	700	629.5	217.9	48.5
7	8	0.1	0.085	119	700	642.4	228.8	61.4
8	8	0.1	0.0567	119	1050	741.0	316.1	303.3
9	8	0.1	0.0567	119	1050	573.2	191.2	63.6
10	8	0.1	0.0567	119	1050	526.8	136.4	38.8
11	8	0.1	0.0567	119	1050	528.1	202.1	71.3
12	8	0.1	0.0567	119	1050	511.3	143.8	25.3
13	8	0.1	0.0567	119	1050	508.7	190.8	58.1
14	8	0.1	0.0567	119	1050	466.9	191.8	35.9
15	8	0.1	0.0476	119	1250	497.2	172.8	48.5
16	8	0.1	0.0476	119	1250	492.3	178.0	63.6
17	8	0.2	0.0476	119	1250	808.9	420.2	541.3
18	8	0.2	0.0476	119	1250	611.2	245.3	100.0
19	2.5	8	0.02	70	1750	529.0	223.7	342.2

Table 25: The cutting force results of the experimental verification

6.3.2 Tool Wear

Tool wear measurement was conducted with Dino-Lite Digital Microscope at the end of each cutting test. As presumed with respect to optimization results, tool life was much longer with higher feed rate and lower spindle speed. The impact of the spindle speed is more dominant than the feed rate for tool life exponentially. In order to maximize MRR in parallel, the selection of the highest feed rate of the tool catalog combined with lower spindle speed will be the optimal solution.



Figure 25: The instrument to measure tool wear: Dino-Lite



Figure 26: Wear status of Tool-life optimized result

Machining Time: 187 seconds

Wear status: 163 microns

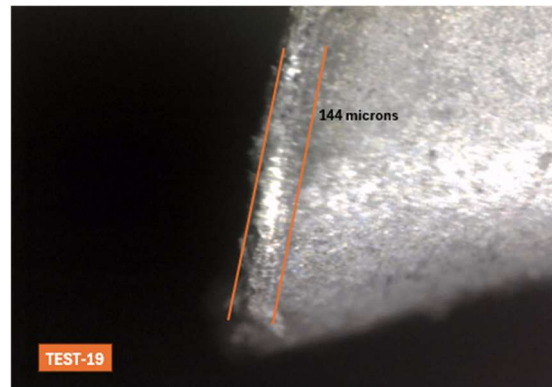


Figure 27: Wear status of MRR-optimized result.

Machining Time: 446 second

Wear Status: 144 microns

6.3.3 Surface Roughness

Surface roughness measurements have been conducted with KTaylor Hobson – Form Talysurf 50 as shown in Figure-28. As can be seen in the experiment table in Table-25, final surface generated for tool life extended version is referring to a different parameter set, axial depth and the feed rate were changed to observe the tool wear. Comparing the surfaces of 18th and 19th experiments resulted in the same amount of the form error as 110 microns. The calculated values for these parameters are 0.0169 and 0.0071 mm for the 18th and 19th test respectively.

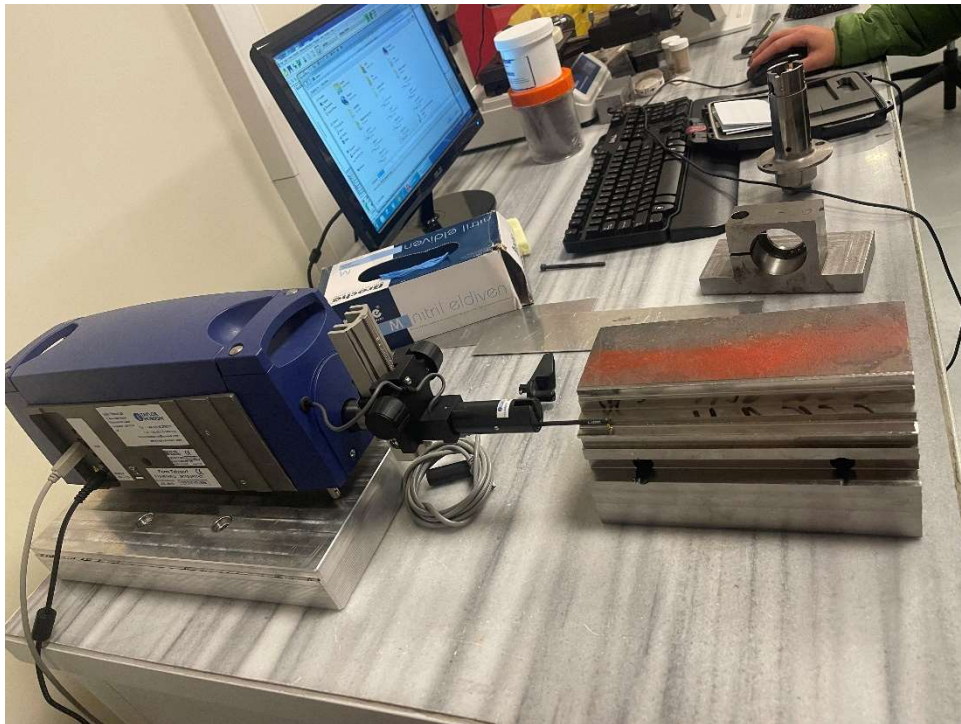


Figure 28: Surface Roughness measurement with KTaylor Hobson – Form Talysurf 50

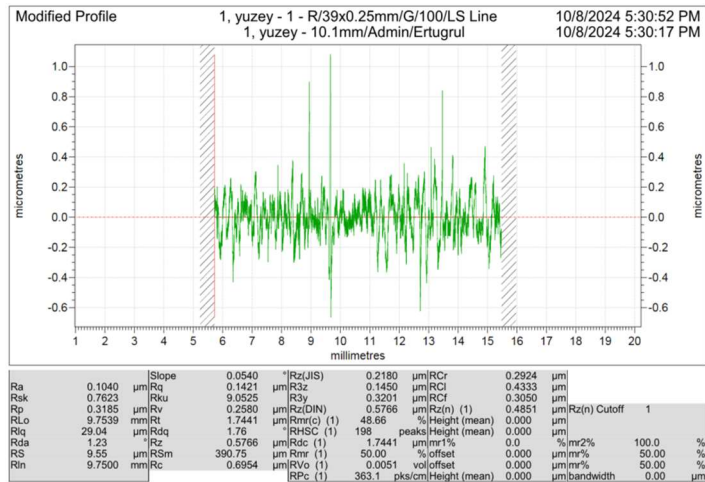


Figure 29: Surface Roughness result for Tool Life maximized solution.

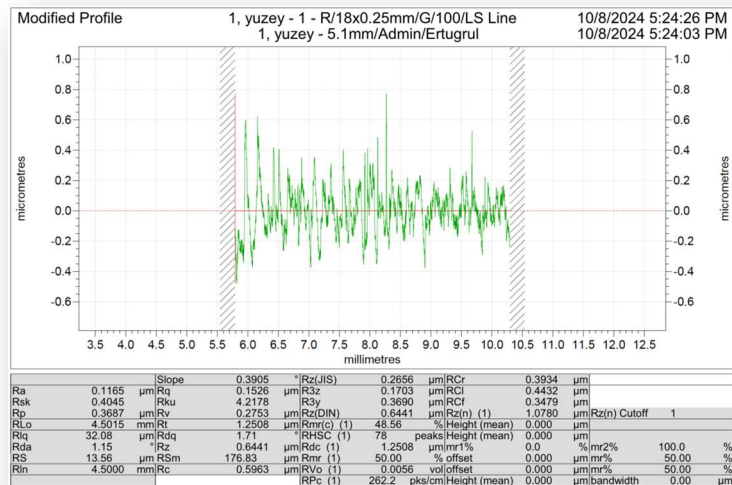


Figure 30: Surface Roughness result for MRR optimized solution.

Table 26 shows that more than one measurement has been evaluated and the average value is considered as results regarding the z values which refer to the surface generation point. Hence, for a back-to-back comparison purpose, the surface roughness of the height $z=0$ has been reported.

	Tool Life-Optimized				MRR Optimized				
test No.	1	2	3	4	1	2	3	4	5
z (height)	0	0	0	0	4	4	4	0	0
Ra	0.0786	0.1368	0.1128	0.1165	0.0729	0.0864	0.0871	0.115	0.104
Average				0.1112			0.08213		0.110

Table 26: Surface Roughness comparison between Tool Life and MRR optimized results

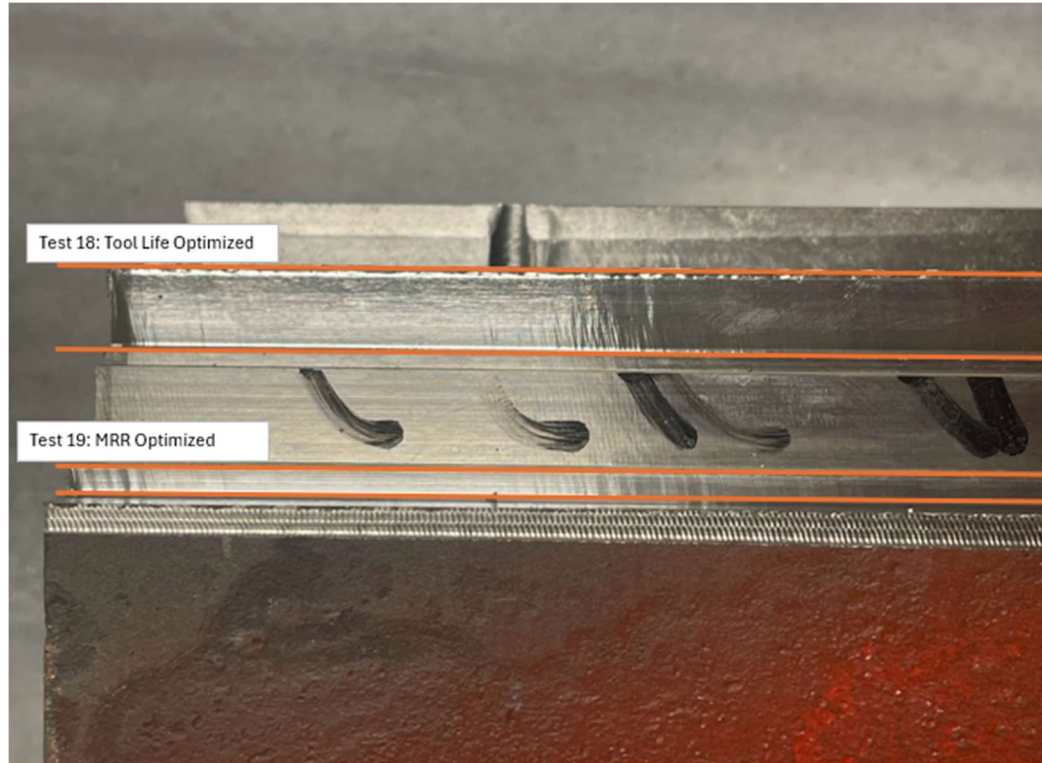


Figure 31: Surface generation and Form Error for two optimized parameters

	Tool Life Maximized	MRR maximized
Machining Time (sec)	187	446
Surface Rougness (microns)	0.111	0.110

Table 27: Surface Roughness comparison

7. Conclusion

This study employed a machine learning-based optimization technique to refine machining parameters for a chatter-free milling operation aimed at maximizing productivity and extended tool life. Productivity definition includes a multi-objective function targeting to maximize material removal rate and tool life while adhering to power/torque limitations and preventing tool breakage. Such an extensive optimization strategy can significantly reduce production costs and improve machining operations' output. For the finishing process, the same multi-objective function was set with different constraints: form error referring to the tolerance requirements of the design and minimum tool life requirement depending on the machining time of the finishing surface not to leave any mismatch line. Cutting forces estimations have used a physics-based machine learning model and used to calculate power, torque, form error, and bending stress. The results for 3 different optimization methodology is available in this study and an experimental verification test set is listed separately.

The study conducted several conclusions:

1. Machine Learning with Gaussian process regression resulted with high performance apart from tool life output so that tool life estimations is using Gradient Boosting approach.
2. Bayesian optimization, compared to Genetic Algorithm and Non-Linear Constrained, has provided a more effective framework for optimizing the objective functions. The solution sets of Bayesian optimization can help better in decision making.
3. Chatter degrades surface quality, reduces tool life, and increases production costs. Since chatter cannot be added to optimization function mathematically, the results need a filtering step with a quick hammer test.
4. Sensitivity analysis showed that feed rate and axial depth of cut significantly affect form error and bending stress. Tooth number, feed rate, and axial depth of cut are primary factors for power; radial depth of cut and feed rate are crucial for torque;

and spindle speed and feed rate most influence tool life. All input parameters equally affect material removal rate (MRR).

5. When the manufacturer wants to achieve higher MRR and higher tool life at equal importance, the feed rate can be set as the maximum tool catalog and the rest can be optimized, respectively. Bayesian optimization is leading better results with respect to genetic algorithm.
6. When only MRR is the main concern, manufacturers can tend to select highest parameters limited by the machine center. Thermal conditions have not been considered in this study, hence the MRR optimized results turned the tool color into red with dry cutting conditions. These parameters are the edge of the cliff for maximum MRR.
7. Explicit weight definition is available only with Bayesian Optimization technique.
8. Each algorithm is developed to give 20 solutions due to chatter filtering step. These 20 solutions additionally refer to different cutting scenarios like pocketing and profiling because if axial and radial depth is replaced vice versa, the optimum solution result will not be affected.
9. When manufacturers will machine large die casts, the minimum tool life for finishing needs to be defined in the optimization problem. Highest MRR objective will tend to list the maximum parameters, however primarily spindle speed, secondarily feed rate must be limited according to minimum tool life requirement. Bayesian optimization performs better results with respect to non-linear constrained approach.

In summary, this study demonstrated that a machine learning-based optimization technique offers a more adaptive and intelligent approach to optimizing machining parameters. By incorporating multiple objectives and constraints, this method provides a comprehensive and practical solution to real-world machining challenges, enhancing productivity and improving the overall quality and efficiency of milling operations.

REFERENCES

- [1] Tekeli, A., & Budak, E. (2005). Maximization of Chatter-Free Material Removal Rate in End Milling Using Analytical Methods. *Machining Science and Technology*, 9, 147 - 167. <https://doi.org/10.1081/MST-200059036>
- [2] Budak, E., & Tekeli, A. (2005). Maximizing Chatter Free Material Removal Rate in Milling through Optimal Selection of Axial and Radial Depth of Cut Pairs. *CIRP Annals*, 54, 353-356. [https://doi.org/10.1016/S0007-8506\(07\)60121-8](https://doi.org/10.1016/S0007-8506(07)60121-8).
- [3] Ghani, J., Choudhury, I., & Hassan, H. (2004). Application of Taguchi method in the optimization of end milling parameters. *Journal of Materials Processing Technology*, 145, 84-92. [https://doi.org/10.1016/S0924-0136\(03\)00865-3](https://doi.org/10.1016/S0924-0136(03)00865-3).
- [4] Budak, E., & Kops, L. (2000). Improving Productivity and Part Quality in Milling of Titanium Based Impellers by Chatter Suppression and Force Control. *CIRP Annals*, 49, 31-36. [https://doi.org/10.1016/S0007-8506\(07\)62890-X](https://doi.org/10.1016/S0007-8506(07)62890-X).
- [5] Merdol, S., & Altintas, Y. (2008). Virtual Simulation and Optimization of Milling Applications—Part II: Optimization and Feed rate Scheduling. *Journal of Manufacturing Science and Engineering-transactions of The Asme*, 130, 051005. <https://doi.org/10.1115/1.2927435>.
- [6] Karandikar, J., Honeycutt, A., Schmitz, T., & Smith, S. (2020). Stability boundary and optimal operating parameter identification in milling using Bayesian learning. *Journal of Manufacturing Processes*. <https://doi.org/10.1016/j.jmapro.2020.04.019>.
- [7] Tansel, I., Arkan, T., Bao, W., Mahendrakar, N., Shisler, B., Smith, D., & Mccool, M. (2000). Tool wear estimation in micro-machining.: Part I: tool usage–cutting force relationship. *International Journal of Machine Tools & Manufacture*, 40, 599-608. [https://doi.org/10.1016/S0890-6955\(99\)00073-5](https://doi.org/10.1016/S0890-6955(99)00073-5)
- [8] Li, J., & Chang, Y. (2018). Development of an Intelligent Optimization System for Machining Parameters Using Machine Learning. *Journal of Intelligent Manufacturing*, 29(6), 1355-1364.

- [9] Bertsimas, D., & Dunn, J. Machine Learning under a Modern Optimization Lens. Dynamic Ideas
- [10] Yan, J., & Li, L. (2013). Multi-objective optimization of milling parameters – The trade-offs between energy, production rate and cutting quality. *Journal of Cleaner Production*, 52(1), 462–471. <https://doi.org/10.1016/j.jclepro.2013.02.034>
- [11] Corson, G., Tyler, C., Dvorak, J., & Schmitz, T. (2024). Minimum cost, stability constrained preform optimization for hybrid manufacturing. *Manufacturing Letters*, 39(C). <https://doi.org/10.1016/j.mfglet.2023.10.004>
- [12] Soori, M., & Asmael, M. (2022). A review of the recent development in machining parameter optimization. *Jordan Journal of Mechanical and Industrial Engineering*, 16(2), 207–219. Retrieved from <https://hal.science/hal-03588524>.
- [13] Snoek, J., Larochelle, H., & Adams, R. P. (2012). Practical Bayesian Optimization of Machine Learning Algorithms. In *Advances in Neural Information Processing Systems* (pp. 2951-2959).
- [14] Joy, T., Rana, S., Gupta, S., & Venkatesh, S. (2019). A flexible transfer learning framework for Bayesian optimization with convergence guarantee. *Expert Syst. Appl.*, 115, 656-672. <https://doi.org/10.1016/j.eswa.2018.08.023>
- [15] Merchant, E., 1945, Mechanics of the Metal Cutting Process I. Orthogonal Cutting and a Type 2 Chip, *Journal of Applied Physics*, 16/5:267-275.
- [16] Krystof, J., 1939, *Berichte uber Betriebswissenschaftliche Arbeiten*, Bd., 12. VDI Verlag.
- [17] E.H. Lee and B.W. Shaffer, 1951, The Theory of plasticity applied to a problem of machining, *Trans. ASME, J. Appl. Mech.*, 18:405–413.
- [18] Palmer, W.B., Oxley, P.L.B., 1959, Mechanics of Orthogonal Machining, *Proc. Instn. Mech. Engrs.*, 173/24:623-638.
- [19] Armarego, E.J.A., Brown, R.H., 1969, “*The Machining of Metals*”, Prentice-Hall.
- [20] Altintas, Y., 2000, *Manufacturing Automation*, Cambridge University Press.
- [21] G. V. Stabler, 1964, The Chip Flow Law and Its Consequences. *Advances in Machine Tool Design and Research*, pp.243-251
- [22] Budak, E., & Özlü, E. (2008). Development of a thermomechanical cutting process model for machining process simulations. *Cirp Annals-manufacturing Technology*, 57, 97-100. <https://doi.org/10.1016/J.CIRP.2008.03.008>.

- [23] Jin, X., & Altintas, Y. (2012). Prediction of micro-milling forces with finite element method. *Journal of Materials Processing Technology*, 212, 542-552. <https://doi.org/10.1016/J.JMATPROTEC.2011.05.020>.
- [24] Ebrahimi Araghizad, A., Pashmforoush, F., Tehranizadeh, F., Kilic, K., Budak, E., Improving milling force predictions: A hybrid approach integrating physics-based simulation and machine learning for remarkable accuracy across diverse unseen materials and tool types, *Journal of Manufacturing Processes*, 114, 92-107, 2024. <https://doi.org/10.1016/j.jmapro.2024.02.001>
- [25] Altintas, Y. (2000). Modeling Approaches and Software for Predicting the Performance of Milling Operations at MAL-UBC. *Machining Science and Technology*, 4, 445 - 478. <https://doi.org/10.1080/10940340008945718>.
- [26] Budak, E. (2006). Analytical models for high performance milling. Part I: Cutting forces, structural deformations and tolerance integrity. *International Journal of Machine Tools & Manufacture*, 46, 1478-1488. <https://doi.org/10.1016/J.IJMACHTOOLS.2005.09.009>
- [27] Kıvanç, E., & Budak, E. (2004). Structural modeling of end mills for form error and stability analysis. *International Journal of Machine Tools & Manufacture*, 44, 1151-1161. <https://doi.org/10.1016/J.IJMACHTOOLS.2004.04.002>
- [28] Lee, Y. J., Yoon, H.-S. (2023). Modeling of cutting tool life with power consumption using Taylor's equation. *Journal of Mechanical Science and Technology* 37 (6) (2023) 3077~3085. <http://doi.org/10.1007/s12206-023-0531-5>
- [29] Altintas, Y., 2000, *Manufacturing Automation*, Cambridge University Press.
- [30] Nemes, J., Asamoah-Attiah, S., Budak, E., & Kops, L. (2001). Cutting Load Capacity of End Mills with Complex Geometry. *CIRP Annals*, 50, 65-68. [https://doi.org/10.1016/S0007-8506\(07\)62072-1](https://doi.org/10.1016/S0007-8506(07)62072-1)
- [31] Wojciechowski, S. Estimation of Minimum Uncut Chip Thickness during Precision and Micro-Machining Processes of Various Materials—A Critical Review. *Materials* 2022, 15, 59. <https://doi.org/10.3390/ma15010059>
- [32] Pashmforoush, F., & Seyedzavvar, M. (2023). A transfer learning-based machine learning approach to predict mechanical properties of different material types fabricated by selective laser melting process. *Proceedings of the Institution of Mechanical*

- Engineers, Part E: Journal of Process Mechanical Engineering.
<https://doi.org/10.1177/09544089231215683>.
- [33] Shahriari, B., Swersky, K., Wang, Z., Adams, R., & Freitas, N. (2016). Taking the Human Out of the Loop: A Review of Bayesian Optimization. *Proceedings of the IEEE*, 104, 148-175. <https://doi.org/10.1109/JPROC.2015.2494218>.
- [34] Altintas, Y., & Budak, E. (1995). Analytical Prediction of Stability Lobes in Milling. *CIRP Annals*, 44, 357-362. [https://doi.org/10.1016/S0007-8506\(07\)62342-7](https://doi.org/10.1016/S0007-8506(07)62342-7).
- [35] T. L. Schmitz, K.S. Smith, *Machining dynamics: Frequency response to improved productivity*, Springer, 2009. <https://doi.org/10.1007/978-0-387-09645-2>.
- [36] Koenigsberger, F. and Tlusty, J. (1967). *Machine Tool Structures-Vol. I: Stability Against Chatter*. Pergamon Press.
- [37] Budak, E. (1994). *The Mechanics and Dynamics of Milling Thin-Walled Structures*. Ph.D. Dissertation, University of British Columbia.
- [38] Altintas, Y., & Budak, E. (1995). Analytical Prediction of Stability Lobes in Milling. *CIRP Annals*, 44, 357-362. [https://doi.org/10.1016/S0007-8506\(07\)62342-7](https://doi.org/10.1016/S0007-8506(07)62342-7).
- [39] Budak, E., & Altintas, Y. (1998). Analytical Prediction of Chatter Stability in Milling—Part II: Application of the General Formulation to Common Milling Systems. *Journal of Dynamic Systems Measurement and Control-transactions of The Asme*, 120, 31-36. <https://doi.org/10.1115/1.2801318>.
- [40] Altintas, Y. (2001). Analytical Prediction of Three-Dimensional Chatter Stability in Milling. *Jsmc International Journal Series C-mechanical Systems Machine Elements and Manufacturing*, 44, 717-723. <https://doi.org/10.1299/JSMEC.44.717>
- [41] Smith, S., Winfough, W., & Halley, J. (1998). The Effect of Tool Length on Stable Metal Removal Rate in High-Speed Milling. *CIRP Annals*, 47, 307-310. [https://doi.org/10.1016/S0007-8506\(07\)62839-X](https://doi.org/10.1016/S0007-8506(07)62839-X).
- [42] Tlusty, J., Ismail, F., and Zaton, W. (1983). Use Of Special Milling Cutters against Chatter, *NAMRC Conference 11, SME*, 408–415.
- [43] Altintas, Y., Engin, S., & Budak, E. (1998). Analytical Stability Prediction and Design of Variable Pitch Cutters. *Manufacturing Science and Engineering*. <https://doi.org/10.1115/1.2831201>.

- [44] Schmitz, T., & Donalson, R. (2000). Predicting High-Speed Machining Dynamics by Substructure Analysis. *CIRP Annals*, 49, 303-308. [https://doi.org/10.1016/S0007-8506\(07\)62951-5](https://doi.org/10.1016/S0007-8506(07)62951-5).
- [45] Schmitz, T., Davies, M., & Kennedy, M. (2001). Tool Point Frequency Response Prediction for High-Speed Machining by RCSA. *Journal of Manufacturing Science and Engineering-transactions of The Asme*, 123, 700-707. <https://doi.org/10.1115/1.1392994>